THE ASTROPHYSICAL JOURNAL, 398:299–318, 1992 October 10

ON THE CAUSES OF TEMPERATURE CHANGE IN INHOMOGENEOUS LOW-DENSITY ASTROPHYSICAL PLASMAS

JACK D. SCUDDER
Laboratory for Extraterrestrial Physics, Mail Code 692, NASA/Goddard Space Flight Center, Greenbelt, MD 20771
Received 1990 July 12; accepted 1992 April 20

ABSTRACT

A kinetic discussion is presented of the temperature changes possible in inhomogeneous, low-density plasmas for a variety of boundary distribution functions that occur in astrophysics. Emphasis is placed on the spatial changes in temperature and their correlations with those of the density caused by time-independent, but spatially varying, conservative potentials; examples from *in situ* space plasma measurements where these effects have been documented are organized by this approach. Where equivalent polytropes are determined, they are shown to have exponents γ greater than, equal to, and less than unity. A graphical proof is provided that decelerating forces produce equilibrium temperatures that are anticorrelated with densities provided that the boundary condition is non-Maxwellian. This proof is extended analytically for a generalized Lorentzian distribution to show that they obey a polytrope relation with $0 < \gamma < 1$. Five factors influence the interactions of a gas with these potentials: (1) the boundary Mach number of the flow, (2) the proximity of the initial velocity distribution to a convected Maxwellian, (3) the relative size of the convection energy and the energy change associated with the potential, (4) the repulsive or attractive nature of the potential, and (5) the collisionality and degree of ionization of the medium. In the presence of spatial variations of the potential energy, general rules for the accompanying temperature profiles are developed. This temperature, the root mean square of the distribution of particle speeds, has a spatial variation for all circumstances except decelerating forces acting on Maxwellian distribution at rest. These changes are observed in numerous *in situ* contexts of space plasmas as well as in laboratory apparatus with charged particle beams. Considering the generality of the argument and the ubiquity of nonthermal phase-space distributions wherever *in situ* space plasma measurements are made, and the inability of residual Coulomb scattering in a fully ionized, inhomogeneous plasma to suppress these effects, these considerations raise new possibilities for the interpretation of remote astrophysical observations with conclusions potentially different from those permitted by classical thermodynamical arguments. These new possibilities occur when the traditional plasma fluid closure/truncation schemes are relaxed to address the consequences of nonnegligible suprathermal populations that are routinely sampled by spacecraft.

Subject heading: plasmas

1. INTRODUCTION

The economy of the fluid description for astrophysical plasmas is clear; the range and correlation of macroscopic variables it can accurately describe is limited, however, by the suitability of the closure and moment truncation approximations assumed. Sometimes closure is imposed on the momentum equation with a polytrope assumption (Chandrasekhar 1939, p. 84) or, alternatively, on the energy equation with Spitzer-Härm (1953) and Braginskii (1965) (SB) or Chapman (1916) and Enskog (1917) (CE) style transport relations. The appropriate moment equation to seek fluid closure for a plasma is unknown; the solution of the chosen level of truncation of the moment equations must be checked a posteriori to demonstrate that it is compatible with the microscopic assumptions that allowed closure. This paper explores equilibrium relations between density and temperature for a fully ionized plasma (FIP) that are more nearly compatible with the thermal inhomogeneity of astrophysical plasma systems. These results are contrasted with those of the polytrope approximation predicated on the nearly infinite collision-frequency approximation and those of the SB method, which postulates a weak gradient system with nearly isothermal equilibrium.

There are three classes of inhomogeneous equilibria that underlie transport approximations: (I) isothermal equilibria enclosed by the same heat reservoir; (II) adiabatic/polytropic equilibria bounded by two different heat reservoirs; and (III) other equilibria with specified moment boundary conditions. Class III is distinguished from the first two classes by its ambiguity concerning the velocity distribution function at the boundaries where the moments are specified. Class III has three different parameter regimes organized by their Knudsen number, K: class IIIa, the SB regime of infinitesimally small K; class IIIb, the Vlasov regime of infinite K with specified boundary conditions on $f(x, v)$; and class IIIc, the Knudsen/Hybrid regime for finite/variable K with particle energy. Classes I–III are usually thought to determine spatial profiles of density N and temperature T that satisfy the relation $d\ln T/d\ln N \geq 0$ unless explicit entropy sources are identified.

Classes IIIa–c represent approaches for class III problems based on the degree of collisionality postulated. Class IIIa is the more traditional astrophysical approach for class III problems using SB transport relations for weak gradient systems, after postulating sufficient assumptions to sustain these closure relations. As is well known (e.g., Cercignani 1975), this class of solutions to the Boltzmann equation represents the "normal" solutions, and they are not a complete set of solutions by any stretch of the imagination. A Vlasov equilibrium of class IIIb

reveals the deformations of the distribution function that free-streaming particles would create; it also illustrates what tendencies the neglected collisions must counteract to achieve local Maxwellians. The Knudsen/Hybrid regime (class IIIc) is the least conducive to analysis of the equilibria outlined; astrophysical plasmas, however, revel in demonstrating that such equilibria are possible. In this paper a new approach in this direction is described and used to achieve initial results, including demonstration of $dT/dN < 0$ behavior in the complete absence of collisions and local entropy production.

The idealized equilibria of class I permit special and even strong gradients in the density, provided that the forces are reversible. The enveloping infinite heat capacity bath sets the Maxwellian character of the velocity space near the boundaries, while the potential ψ associated with the force modifies the number density of the medium in accordance with the Boltzmann factor, viz.,

$$f(x, v) = \exp\left[-\frac{\psi(x) - \psi(x_0)}{kT_0}\right] f_M(x_0, T_0, v) . \quad (1)$$

Fortuitously, equation (1) is the collisionless and collisional solution to the posed problem with the specified boundary conditions. Since $f(x, v)$ in equation (1) is separable between x and v dependence, being proportional to a local Maxwellian, f_M, it clearly satisfies the collision operator. Equation (1) is also a Vlasov solution, since it may be rearranged to demonstrate that $f(x, v)$ is just a function of the boundary conditions and the total (kinetic plus potential) energy. The spatially uniform equilibria of this class represent the force-free limit of equation (1). *In either case the scale length of the temperature gradient is infinite, while the collision frequency within the interior of the solution is not prescribed; accordingly, for this class the FIP Knudsen number, $K \equiv \lambda_{mfp}/L$, is vanishingly small, and uniformly so with energy, regardless of the collision frequency.* This class of solutions leaves the temperature passive and unmodified regardless of the density variation ($d \ln T/d \ln N = 0$).

The adiabatic closure approximation of class II is the result, in lowest order in the inverse collision frequency, of Hilbert's perturbative distribution function solution of the Boltzmann equation (Cercignani 1975). The kinetic derivation assumes that the distribution function is kept locally Maxwellian by an arbitrarily large collision frequency. Since transport modifications to the distribution function are signatures of persistence due to free-path effects, it is clear that an infinitely large collision frequency can preempt transport effects uniformly in energy even in a FIP, thus "localizing" the kinetic distribution. By *postulate* the energy-dependent Knudsen number, $K(E)$, is vanishingly small because $K(E) = \lambda_{fp}(E)$ is vanishingly small at any energy, while the scale of spatial gradients remains finite. The adiabatic relation, $V \cdot \nabla \ln (P/\rho^{5/3}) = 0$, can thus be consistent with spatial gradients of density and temperature along streamlines. However, the gradients have a special *fixed* relationship given by

$$\frac{d \ln T/ds}{d \ln N/ds} = \frac{2}{3} > 0 ,$$

where ds is along the streamline: when the density changes, the temperature follows in the same direction.

The polytropic relation, $V \cdot \nabla \ln (P/\rho^{\gamma}) = 0$, represents a macroscopic attempt to model "convective equilibria" thought to be relevant in atmospheric layers where heat is transmitted by advection rather than conduction (cf. Chandrasekhar 1939, p. 84). These phenomenological treatments with $1 \leq \gamma \leq 5/3$ *postulate* the form of local changes in pressure that attend changes in specific volume in the presence of local heat exchange. Parker (1958, 1964a) and others have used this ad hoc simplification to advantage in exploratory models of the solar wind expansion with distributed heat deposition. *The necessary scattering mechanisms that can sustain a polytropic equation of state* for a simple plasma without internal degrees of freedom *are unknown.* This approach leads to the result $d \ln T/d \ln N = \gamma - 1 \geq 0$.

Two regimes for strictly adiabatic behavior are well known: (1) nonzero subsonic flow with conditions on transport signatures and (2) extremely supersonic flow with essentially no constraints on transport signatures. In subsonic flow adiabaticity follows from the steady state internal energy equation

$$V \cdot \nabla \ln\left[\left(\frac{P}{\rho}\right)^{5/3}\right] = \frac{2}{3P}(-\nabla \cdot q + J^* \cdot E^* - \mathbf{S}:\nabla V) ,$$

by *postulating* that the electric dissipation, the viscosity, and the $\nabla \cdot q$ are small. All the postulated transport signatures can be made small by requiring that the free path for transport be asymptotically small at all energies as in the case of a very large collision frequency. An example of such a system is a flowing neutral high-density, low-temperature gas. Alternatively, in the supersonic regime, if the time for the center of mass to traverse the shortest macroscopic scale length is short compared with the time for energy transfer *of all species*, then the total pressure evolves along a streamline as an adiabatic fluid, regardless of the degree of collisionality or strength of the dissipation, viscosity, or divergence of the heat flux. This corresponds to dividing the internal energy equation through by $|V|$, which then compares all the finite free-path transport signatures to the enthalpy flux, PV; when this ratio gets small, the adiabatic relationship on the one-fluid pressure follows. Class I solutions appear to meet the prerequisites for suggesting the adiabatic equation of state (since $q = 0$, $\nabla V = 0$, $J^* = 0$), except that class I solutions do not have streamlines. In this regime $P/\rho^{5/3}$ is not constrained as it otherwise would be, if $|V|$ did not vanish.

The third transport regime (class III) reflects the more typical problem is astrophysics: an inner and outer boundary condition specified on density, mass flux, pressure, and energy flux. The nearest stars shape astrophysical systems by their gravity and thermally drive them in an asymmetrical way. The question then is, what does the interior spatial profile look like? Neither the isothermal approximation of class I nor the polytropic approximation of class II is defensible, and usually some form of the SB (class IIIa) or Vlasov (class IIIb) scheme for the problems in class III is attempted.

Unlike Hilbert's "adiabatic" expansion (class II) for the *solution*, $f(x, v)$, to the Boltzmann equations, the SB approach (class IIIa) attempts to expand the integro–partial differential Boltzmann equation and replace it with a finite set of coupled equations for the velocity space *moments of the solution*, $M_\eta \equiv \int f v^\eta d^3v$, of the Boltzmann equation. The SB closure/truncation approach relates the collisional modifications of energy and momentum to lower order moments. This approach presumes that the differences of the actual distribution function and a local Maxwellian distribution (of equal density and pressure) are insignificant for all velocity moments above the third. In particular, the level of the suprathermal particles above $v \simeq 3(2kT/m)^{1/2}$ (above energy $E'' = 9kT$) is

presumed to be that predicted by the local Maxwellian distribution. This approach is most useful when a few of the lowest order moments can approximate the solution to the original Boltzmann equation. The Navier-Stokes equations represents the lowest order truncation of class III, and the distribution function that solves the Boltzmann equation involves N, T, and V as well as the gradients of density and velocity. At the next level the internal energy equation with Fourier's heat transfer is obtained and heat is predicted to flow from higher to lower temperatures. The reconstruction of the distribution function in this case becomes a function of $\{N, T, V\}$ and all their first derivatives. Attempts have been made to consider the fourth level in the moment hierarchy (Cuperman, Weiss, & Dryer 1980); this formulation develops an evolutionary equation for the suprathermal excess relative to that of the local Maxwellian, requires an ad hoc closure assumption concerning the fifth moment, but it does not accurately describe the observed electron distributions at 1 AU, possessing negative probability density within some regions in the velocity space radius $\sim 3(2kT/m)^{1/2}$.

The usual (WKB) multiple scales approach for CE–SB closure and transport neglects the global scale variation of the moments while focusing on the scale of the mean free path for collisions. The spatial profile is then found as a resummation of these local partial differential equations that constrain the unknown moment relations. Such an approach *has* been used with success in neutral gases, where the uniform bound on the energy dependence of the free path (cf. Fig. 1) allows the computation of the necessary and sufficient conditions for the subsequent CE transport expansion to converge rapidly ($K < 1$); its predictions and experiment agree remarkably well, even for finite, as contrasted with infinitesimal, gradients. However, the strong speed dependence of the free path, $\lambda_{fp}(E)$, in a FIP (cf. Fig. 1) does not lend itself *at any density* to the CE style insulation of the microscopic scale from the macroscopic one; this is especially true at suprathermal energies (Scudder & Olbert 1979a), which, by dimensional analysis alone, control the magnitude and sense of the heat flow.

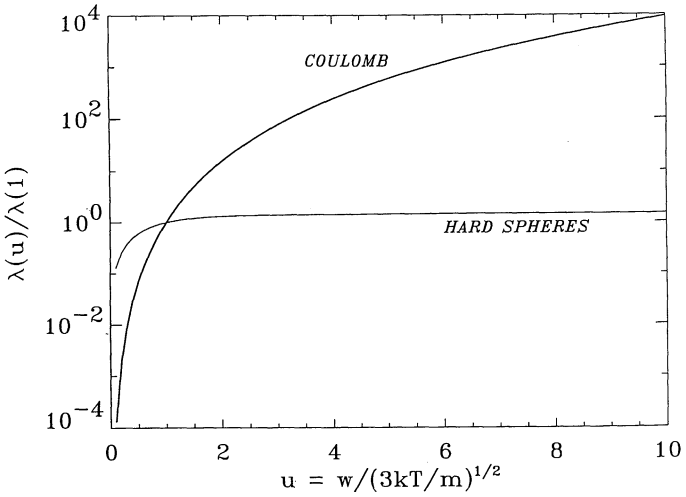

FIG. 1.—Speed dependence of free path. Comparison of the speed dependence of neutral (Tait 1886) and fully ionized Coulomb (Rosenbluth, Macdonald, & Judd 1957 or Rossi & Olbert 1970) mean free paths. Note that a uniform bound on the free path exists in the case of hard sphere scattering, while one does not exist for the Coulomb scattering.

The CE–SB procedure is still, however, a one-term Maclaurin expansion in the Knudsen number , $K(\lambda) = \lambda/L$, where λ is the free path for scattering and L is the shortest scale length over which the lowest order moment quantities vary. The size of *all* the moments of the solution $f(x, v)$ are assumed at each spatial location to be close to the size of the same moment of the Maxwellian of equivalent density and temperature. In order that finite collision frequencies can be allowed, the scales, L_η, of all lowest order moment quantities are supposed large. To keep the Knudsen parameter small with finite, rather than nearly infinite, L_η, these schemes rely on the free path λ ($\propto 1/\nu$) being suitably small. With a finite spatial scale, L_η, the strongly increasing free path with speed in a FIP (cf. Fig. 1) makes it difficult at any finite density to keep the free path small, sufficiently uniformly in energy, across the distribution function. Consistency of the SB approach of the CE method is enforced presupposing ultraweak thermal gradients (cf. Braginskii 1965) to make K uniformly small enough (Scudder & Olbert 1983). The SB approaches are mathematically and physically self-consistent, *provided* (1) that collisions are sufficiently vigorous to maintain a spatially homogeneous Maxwellian velocity distribution of random velocities in lowest order; (2) that the gradients of all the macroscopic moment variables are suitably weak, including being nearly isothermal, with scale lengths much larger than the scale length for momentum exchange of *all* particles that "determine" the macroscopic variables of interest; and (3) that the fluid flow is ultra-subsonic (Scudder & Olbert 1983). The self-consistency of these closure approximations is compromised if *any of these* interlocking provisos are not fulfilled by the fluid solution generated from the equations derived under this closure assumption. Shock layers and the acceleration regions of fully ionized stellar winds are examples of astrophysical regimes that do not fulfill these interlocking conditions for SB closure. Another example of a solution of the Boltzmann equation not accessible from the SB approach is the class I solutions with strong variations in the potentials, and hence the density, which violate the weak gradient premise of the CE–SB approach.

Realistic FIP astrophysical systems are not, however, isothermal, because they are not enclosed by isothermal heat baths. They cannot be described in the WKB way as perturbation expansions about local Maxwellians of a common temperature. The transport in such systems is global until an omnipresent mechanism can be found that curtails the range of the suprathermal particles to be shorter than the gradient scales in the macroscopic variables, or the expansion velocity becomes extremely supersonic with respect to the electron thermal speed. Scudder & Olbert (1979a, b) illustrated examples of "global" communication for a thermally inhomogeneous model of the solar wind expansion. In these calculations the thermal/suprathermal dichotomy of the near 1 AU electron distribution function (cf. Feldman et al. 1975) was argued to reflect two classes of particles: (1) those that scattered locally and would be considered consistent with a WKB approach and (2) those which were last in collisional contact with particles many mean free paths away that globally determined the local suprathermal population. This work also illustrated the generic local Coulomb window above $2.6(2kT/m)^{1/2}$ that made such nonlocally determined distributions a natural occurrence from the streaming effects of the kinetic equation and lowest order spatial inhomogeneity of the temperature. Since these global particles were the essential determinants of the local heat flux, it was concluded that local heat laws of the SB type

at 1 AU were probably not possible. These authors also suggested that such nonlocal effects which promote suprathermal populations might play a crucial role in the energy supply for the solar wind near the thermally inhomogeneous coronal base, as followed up in quantitative detail by Scudder & Olbert (1983) and further by Olbert (1983) as critically reviewed by Shoub (1989).

Scudder & Olbert interpreted the simultaneous presence of "global" and "local" particles scattered on scale lengths large and small compared with the local mean free path as the fingerprint of the speed dependence of the Coulomb cross section and the increasing temperature between the Sun and the observer. The transport signatures in thermally stratified FIPs can only be fully determined by knowledge of the distribution of phase-space density and forces across the system and the local Knudsen number of the typical particles.

A WKB–style plasma closure approximation (as developed in Chapman & Cowling 1970) may or may not be consistent with the underlying effects of the streaming side of the transport equation. The polytrope closure rule is a local functional relationship; the SB rules relate higher order moments to gradients of other macroscopic variables and may be thought of as proximate, as in the first term in a Maclaurin series, e.g.,

$$\boldsymbol{Q} = \boldsymbol{Q}^{(0)} + \boldsymbol{Q}^{(1)} + \boldsymbol{Q}^{(2)} + \ldots ,$$

$$\boldsymbol{Q} \simeq 0 - \kappa \nabla T + \text{higher order terms} ,$$

since it is an expansion about a lowest order system that has neither heat flow, viscosity, nor ohmic dissipation. Local relationships between state variables such as polytropes or local gradient relationships between state variables constitute very restricted functional types of closure; such descriptions are possibly insufficient to close the fluid equations with precision when global effects permitted by the "Coulomb window" occur at suprathermal energies. There is always some energy for which this "nonlocal" or "global" effect is dominant; if present, such populations will always have more influence on the higher plasma moments whose behavior at the level of closure can be most important! It has already been shown (e.g., Scudder & Olbert 1979a, b) that the streaming, global effects of the left-hand side of the transport equation can influence, if not dominate, the appearance of the locally observed distribution function and hence some, if not all, of its moments. The size of this influence depends on the energy regime where this "global" leakage dominates the local distribution function. Near 1 AU, for example, the global suprathermal electrons contribute $\simeq 30\%$ of the pressure and 6% of the density (Feldman et al. 1975) and almost completely determine the heat flux (Montgomery et al. 1968; Ogilvie, Scudder, & Sugiura 1971b).

There will always be a "window" above which the remote extremes of the plasma system will be quasi-ballistically connected to the local microstate (Scudder & Olbert 1979a). There is now widespread agreement (Scudder & Olbert 1979a, b, 1983; Shoub 1982, 1983, 1989; Delettrez 1985) that $K(\lambda_{\rm mfp}) < 10^{-2}$ is probably *necessary* for an accurate description of a fully ionized plasma with nearly Maxwellian boundary conditions. However, the determination of the local value of $K(\lambda_{\rm mfp})$ *sufficiently* small to ensure that the perturbative SB heat law accurately predicts the size of the heat flow, *independent* of the boundary conditions that the Boltzmann equation permits to flow, is a very difficult question without a complete answer. Initial attempts to comment on this issue by Scudder & Olbert (1979a, 1983), Olbert (1983), and Shoub (1982, 1983, 1989) suggest that *both* the spatial contrast of the phase-space density across the connected plasma volume and the local collisionality of the gas will play a role in answering this question (cf. Scudder 1992a, hereafter Paper II, where $K \leq 10^{-6}$ is suggested as necessary in the solar transition region!).

For problems in class III the appropriate choice for the boundary velocity distribution function is also a difficult matter. As usually posed, the SB problem represents a perturbation expansion for the moments of the distribution function, where the lowest order distribution function is a Maxwellian with the Knudsen number as the expansion parameter. To be a useful approach, the *boundary conditions are usually assumed to be nearly Maxwellians to avoid solving the Boltzmann equation for a kinetic layer* (Cercignani 1975), which would "match" the more complicated boundary velocity distributions to a "moment" description suitable between the boundaries. Under this *assumption* Fourier's law $\boldsymbol{Q} = -\kappa \nabla T$ is retrieved embedded in the full energy equation. The approach truncates the infinity of moments required for the Boltzmann equation, usually stopping at level 2, which is the pressure tensor; truncation at level 3 *implies an assumption* that fourth and higher order moments relative to those implicit in a Maxwellian are unimportant in the particular problem at hand and implies a restriction on the boundary data usually adopted. However, the third moment (energy flux) driving most astrophysical systems is usually substantial, as is the fourth moment, which is the first moment to quantify the number of suprathermal particles relative to the suprathermal population suggested in a Maxwellian. This truncation artificially ignores the implication of an "excess" in the suprathermal population in the boundary conditions. The closure approximation of SB presupposes that the third moment ($\boldsymbol{q}$) is both small *and* related to the lower order moments by Fourier's law, $\boldsymbol{q} = -\kappa(T)\nabla T$.

This paper explores the consequences of nonthermal boundary conditions on problems of class III discussed above via a Knudsen/Hybrid scheme (class IIIc). A companion paper in this issue of the journal (Scudder 1992a, hereafter Paper II) examines the suitability of these results for a description of the solar transition region between the higher chromosphere and the low corona.

2. APPROACHES TO TRANSPORT AND THE NEW HYBRID APPROACH

The kinetic transport equation governs the evolution of the probability distribution function

$$\frac{Df}{Dt} = \nu(v) * \delta(f) , \tag{2}$$

where the "streaming" term (D/Dt), defined as

$$\frac{Df}{Dt} \equiv \frac{\partial f}{\partial t} + \boldsymbol{v} \cdot \frac{\partial f}{\partial \boldsymbol{x}} + \boldsymbol{a} \cdot \frac{\partial f}{\partial \boldsymbol{v}} ,$$

contains the effects of time dependence, of spatial inhomogeneity, and of the coherent macroscopic forces; the right-hand side of equation (2) contains the effects of collisions separated into an effective collision frequency, ν, and a scattering operator functional, δ, of the distribution function.

The CE–SB perturbative techniques are related approaches for closure of neutral gases and fully ionized plasmas, respec-

tively. In lowest order the CE method assumes that the distribution function is identically time-independent, spatially uniform, and is a solution for all $\boldsymbol{x}$ of the scattering operator $[\delta(f^{(0)}) \equiv 0]$; simultaneously, the left-hand side of the kinetic equation is satisfied provided that the distribution function is a local Maxwellian at the same temperature as that of the enveloping heat bath as in equation (1) with a spatially uniform potential. In this way equation (2) is satisfied in lowest order as indicated in equation (3a):

Chapman-Enskog (neutral gases) $(K < 1)$:

$$\begin{array}{ccccccc} \dfrac{\partial f^{(0)}}{\partial t} + \boldsymbol{v} \cdot \dfrac{\partial f^{(0)}}{\partial \boldsymbol{x}} + \boldsymbol{a} \cdot \dfrac{\partial f^{(0)}}{\partial \boldsymbol{v}} \equiv \dfrac{Df^{(0)}}{Dt} = \nu * \delta f^{(0)} \equiv \nu(v) * \delta(f^{(0)}) . \\ \equiv 0 \quad \equiv 0 \quad \equiv 0 \quad 0 \quad 0 \quad \neq 0 \quad \equiv 0 \end{array} \tag{3a}$$

The corrections to the distribution function are then computed as driven by the slight gradients in n and T, as permitted by the finite collision frequency. This is a perturbation expansion for the distribution function with the Knudsen number $K(\lambda_{\rm mfp})$ defined as $\lambda_{\rm mpf} \nabla \ln M_\eta$, where M_η is the macroscopic variable with the shortest scale length; the perturbation approach presupposes that $\lambda_{\rm mfp} \nabla \ln M_\eta = O(K)$ for *all* macroscopic variables that characterize the equilibrium. In equation (3a) this is emphasized by presupposing that the zeroth-order distributions are spatially uniform in all macroscopic variables.

In the original Chapman (1916) and Enskog (1917) approaches for neutral gases, the collision free path, $\lambda_{\rm mfp}$, is not a strong function of energy, never much larger at any energy than its value for the particles of the most probable speed, w_T (cf. Fig. 1). Thus, if $K(\lambda_{\rm mfp})$ is perturbatively small, then $K(\lambda(w))$ is also small for any random speed w. When the CE approach was used for the fully ionized plasma problem, the strong speed dependence of the collisional free path and, hence, Knudsen number (cf. Fig. 1) required explicit "attention." The SB form of equation (3a) is given in equation (3b) for a fully ionized plasma.

Spitzer-Braginskii fully ionized plasma $(K < 10^{-2})$:

$$\begin{array}{lccc} & \dfrac{\partial f^{(0)}}{\partial t} + \boldsymbol{v} \cdot \dfrac{\partial f^{(0)}}{\partial \boldsymbol{x}} + \boldsymbol{a} \cdot \dfrac{\partial f^{(0)}}{\partial \boldsymbol{v}} & & \\ E \le E' : & \equiv 0 & \equiv 0 & \equiv 0 \\ E \ge E' : & \equiv 0 & \equiv 0 & \equiv 0 \end{array}$$

$$\begin{array}{cccc} \equiv \dfrac{Df^{(0)}}{Dt} = \nu * \delta f^{(0)} \equiv \nu(v) * \delta(f^{(0)}) . & & & \\ 0 & 0 & \neq 0 & \equiv 0 \\ 0 & 0 & \simeq 0 & \equiv 0 \end{array} \tag{3b}$$

For a FIP the collision term at high energy is small for two separate reasons: first, the absence at high energy of effective collisions makes the situation at suprathermal energies more Vlasov-like than collisional; and, second, the Maxwellian $f^{(0)}$ zeros the collision operator at high energy by its speed dependence independent of the small number of collisions. Because the collisions at high energy are not as effective at localizing the particles by scattering as at energies below E', the velocity distribution at distances farther than $\lambda_{\rm mfp}$ end up shaping the local distribution function at these suprathermal energies in global ways (Scudder & Olbert 1979a) that are impossible in a neutral gas where the mean free path has an energy-independent upper bound.

Reconciling the behavior of the *probability* distribution with the trajectories of the individual particles can resolve apparent paradoxes. In a FIP a semi-infinite interval in energy of particles above $E' \simeq 7kT$ always exists for *any* finite collision frequency that will not, with high probability, scatter while traversing the last thermal mean free path, $\lambda_{\rm mfp}$, of its trajectory (Scudder & Olbert 1979a, b). This is also true in a spatially uniform FIP: individual *particles* above E' *do* have a range between collisions long compared to $\lambda_{\rm mfp}$. However, if the distribution function is everywhere the same Maxwellian, this ballistic behavior does not invalidate the SB perturbation approach, since such a *probability function* is a solution of the Df/Dt side of the kinetic equation and the *particle* free streaming does not transport corrections to the *pattern* of the velocity probability distribution function. That is, the Maxwellian pattern of particles, $f_{\rm M}^{(0)}$, is consistent with weak transport modifications even if some particles have ballistic ranges longer than $\lambda_{\rm mfp}$, provided that the *system* remains as per the SB premise: spatially uniform in all macroscopic variables in lower order. Since $\nabla \ln M_\eta^{(0)} = 0$ in a SB FIP, the growing, strong speed dependence of $\lambda(w)$ does not cause the expansion Knudsen parameter to necessarily be extremely large if infinitesimal gradients in $M_\eta^{(1)}$ are the results of the transport modified fluid solution. However, finite lowest order temperature gradients require considerable more care, especially for a fully ionized plasma.

For neutral gases (Fig. 1) there is a uniform bound in energy on the ballistic motion of individual particles at any density. *All* the different random speed neutral particles scatter within $O(\lambda_{\rm mfp})$. If the scale length of the gradients of macroscopic variables is long compared with this length, the finite versus the infinitesimal gradient results of CE are equally valid in the usual WKB approximation. At room temperature $\lambda \simeq 10^{-7}$ cm, and small "macroscopic" dimensions of 10^{-4} cm appear suitable for this WKB approach. In the solar wind, for example, the λ can easily be ~ 1 AU, clearly large compared with the gradient scales of the wind itself. For a FIP, however, the energy bound on the free path is *not* independent of particle energy (Fig. 1). This Coulomb "window" to the global scale above $E' \simeq 7kT$ causes the lowest order distribution that is in equilibrium with the inhomogeneous temperature profile of an asymmetrically heated plasma to have signatures of the entire system to which it is magnetically connected (Scudder & Olbert 1979a, 1983; Olbert 1983). These global signatures are the pervasive suprathermal tails, which are not perturbative corrections to local Maxwellians; they exist because of a finite rather than infinitesimal temperature jump across the system. SB as a mathematical perturbation approach for a FIP collapses for finite gradients in macroscopic variables (Scudder & Olbert 1983). The exponential atmosphere *solution* of the Boltzmann equation (not a perturbative approximation!) (eq. [1]) demonstrates that arbitrarily large density gradients are compatible with isothermal local Maxwellian distributions throughout the system that do not have overpopulated suprathermal tails. However, when there is a temperature variation supposed across the system as in the calculations of Scudder & Olbert (1979a) and Olbert (1983), then the suprathermal tails come booming through in superposition with a local population. In this sense the FIP plasma with finite thermal gradients immediately develops a strong global sensitivity that is totally absent in the accurate one-term Maclaurin series

description of neutral gas transport provided by CE. This sensitivity, when coupled with an asymmetrical energy supply of astrophysical FIPs, provides an explanation for the ubiquitous nonlocal suprathermal tails on $f(x, v)$ that are routinely observed.

DeGroot & Mazur (1984, p. 138) conclude that when strong departures from a local Maxwellian distribution occur, the usual SB forms of the heat law and the form of thermodynamic expectations (e.g., heat flowing only from hot to cold) that derive from them no longer apply. When such global phenomena can occur, the additional ad hoc assumption of a local equation of state or closure scheme may preempt effects permitted in nature whose description requires the more fundamental kinetic equation of transport. One of the preempted effects for nonthermal boundary conditions discussed in this paper is a new consequence of *velocity filtration*, which underlies the exponential atmosphere. When velocity filtration occurs, the density and temperature are spatially anticorrelated, provided that the boundary assumptions allow for a nonthermal distribution function.

The opposite extreme from the small Knudsen regime of SB is the infinite Knudsen regime of the Vlasov, or collisionless, approach. Under the Vlasov approximation the kinetic equation is satisfied by counteracting the configuration and velocity space gradient terms of the left-hand side of the transport equation while ignoring the terms on the right-hand side indicated in equation (4):

Vlasov (collisionless) $(K \rightarrow \infty)$:

$$\begin{array}{ccccccc} \dfrac{\partial f^{(0)}}{\partial t} & + \boldsymbol{v} \cdot \dfrac{\partial f^{(0)}}{\partial \boldsymbol{x}} & + \boldsymbol{a} \cdot \dfrac{\partial f^{(0)}}{\partial \boldsymbol{v}} \equiv \dfrac{Df^{(0)}}{Dt} & = v * \delta f^{(0)} \equiv \nu(v) * \delta(f^{(0)}) . \\ \equiv 0 & +\zeta & -\zeta \quad 0 & 0 \quad \equiv 0 & \neq 0 \end{array} \tag{4}$$

While the lowest order Vlasov distributions are not necessarily solutions of the collision operator ($\delta f^{(0)} \neq 0$), collisions are so weak on the scales in question that the right-hand side of the kinetic equation is negligibly small for any normalizable distribution function. The possible solutions in the regime are those positive, normalizable, but otherwise general, functions of the constants of the motion which zero the Liouville continuity equation $Df/Dt = 0$. In general, such solutions will have compensating configuration and velocity space gradients that are consistent with the structure of the forces experienced by the particles and boundary condition assumed. Collisionless shocks, sheaths, and other abrupt transitions (e.g., magnetohydrodynamic [MHD] boundary layers) can be studied in this way when the free path for *all* the particles is long compared with the scale length of the structures.

The isothermal exponential atmosphere is a "bridge" between class I and class III solutions of the Boltzmann equation, on the one hand, and the "Hybrid" approach to be developed next. The density profile of the isothermal exponential atmosphere derived by Maxwell (1873) and Boltzmann (1875) has the form

$$n(x) = n(x_0) \exp\left[- \frac{\psi(x) - \psi(x_0)}{kT_0} \right], \tag{5a}$$

where $\psi(x)$ is the gravitational potential in Maxwell's case, the negative gradient of which is the force experienced by each particle. T_0 is the uniform temperature. Maxwell also showed that the velocity distribution function in the exponential atmosphere (EA) is given by the now famous Maxwellian distribution,

$$f^{\mathrm{EA}}(x, v) = \frac{n(x_0)}{(2\pi k T_0/m)^{3/2}} \exp\left[- \frac{\psi(x) - \psi(x_0)}{kT_0} \right] \times \exp\left(- \frac{mv^2}{2kT_0} \right), \tag{5b}$$

or

$$f^{\mathrm{EA}}(x, v) = \exp\left[- \frac{\psi(x) - \psi(x_0)}{kT_0} \right] f_{\mathrm{M}}(x_0, T_0, v) . \tag{5c}$$

Equation (5c) emphasizes the special self-similarity and x-v separability properties of the Maxwellian in an attractive potential: $f(x, v)$ is proportional to the same Maxwellian velocity space function, f_M, at all locations in space.

Although the EA solution can be derived from the *collisionless* Boltzmann equation, it was originally derived by Maxwell for the Earth's collisional neutral atmosphere. A digest of the essential aspects of this particular solution indicates that f^{EA} zeros both the homogeneous and inhomogeneous terms separately. Clearly the space of solutions for the Vlasov equation ($Df/Dt = 0$) is broader than the spatially varying Maxwellian of equation (5*c*). Any function of the constants of the motion would solve the Vlasov equation; it is the collision operator that selects the appropriate one of those compatible with the boundary conditions. If the scattering frequency were independent of speed, or nearly so, and the system enclosed in an isothermal infinite capacity heat bath, then f^{EA} would be the only spatially inhomogeneous profile that was close to satisfying the kinetic equation. Another possibility occurs, however, when the effective collision frequency varies strongly with particle speed as does the Coulomb cross section; the Hybrid approach for this problem is discussed next.

The Hybrid approach (introduced in this paper) is useful for the case of interactions with decelerating forces and finite temperature gradients of asymmetrically heated/cooled astrophysical systems with arbitrary scales. This approach addresses free streaming and collisions in different parts of the distribution function and at the same time retains finite spatial gradients and acceleration in lowest order. The scheme for satisfying the kinetic equation in this approach is outlined in equation (6):

Hybrid approach $[K(E < E') < 1; K(E > E') > 1 \rightarrow \infty]$:

$$\begin{array}{lccc} & \dfrac{\partial f^{(0)}}{\partial t} & + \boldsymbol{v} \cdot \dfrac{\partial f^{(0)}}{\partial \boldsymbol{x}} & + \boldsymbol{a} \cdot \dfrac{\partial f^{(0)}}{\partial \boldsymbol{v}} \\ E \leq E': & \equiv 0 & +\zeta & -\zeta \\ E > E': & \equiv 0 & +\xi & -\xi \end{array}$$

$$\equiv \frac{Df^{(0)}}{Dt} = v * \delta f^{(0)} \equiv \nu(v) * \delta(f^{(0)}) . \tag{6}$$

$$\begin{array}{cccc} 0 & \simeq 0 & \neq 0 & \simeq 0 \\ 0 & \simeq 0 & \simeq 0 & \neq 0 \end{array}$$

The Hybrid approach exploits the quadratic smallness of the FIP collision term noted for $E > E'$ in the SB approximation of equation (3b); the kinetic equation for a FIP in lowest order does *not* require a Maxwellian velocity distribution function at energies above E'. That situation in SB arose so as to be consistent with the small departure from the isothermal equilibrium

postulate *and* the Maxwellian boundary conditions with the enveloping heat bath. For the fully ionized plasma hybrid (FIPH) scheme the high-energy portion of the velocity distribution is virtually unmodified by local collisions in lowest order, while the lower energy *particles* may be rearranged by scattering even though their *pattern*, $f^{(0)}(E < E')$, is essentially unmodified by such activity. *The essential reason that the EA solution works as both collisional and collisionless solution is that the characteristics of the left-hand side deform the Maxwellian boundary distribution in a way that keeps the distribution function a Maxwellian, which is the special function that zeros the collision operator. At suprathermal energies the EA solution zeros the collision operator as indicated in equation (4) twice over: once by the dearth of collisions and once by the special velocity space functional dependence by being a Maxwellian.* In the FIPH approach, the view is taken that the boundary conditions provided by the low-level moments of the distribution function are not sufficient in number to preclude the suprathermal population from being present at the boundary of the problem of class III above. If prototype boundary functions, f_κ, can be found that are quasi-Maxwellian at low energy and self-similar at low energy under the action of Df_κ/Dt, then such prototypes would allow a lowest order attack on the influence of the suprathermal tails on the spatial profile of class IIIc solutions because the weakness of collisions at high energies counteracts, in lowest order, f_κ not being a null eigenfunction of the scattering operator. The FIPH approach reduces to studies of the $Df_\kappa/Dt = 0$ consequences for lowest order boundary distributions that at low energy nearly zero the collision operator $[(\delta f_\kappa^{(0)}(E < E') \simeq 0]$ but at high energy are unconcerned by this requirement given the numerical weakness of the collisions for $E > E'$. In this way the FIPH approach generalizes the exponential atmosphere; it can discuss slight departures from isothermal equilibrium as well as potentially nonthermal distributions that satisfy $Df_\kappa^{(0)}/Dt$. If the collision frequency is reduced further, or system scales made shorter, the FIPH problem goes over into a Vlasov problem of class IIIb with a restricted rather than arbitrary boundary condition.

It remains to the shown that a prototype boundary velocity distribution exists that has the correct properties required of the FIPH scheme: can a streamed distribution function that solves $Df_\kappa/Dt = 0$ retain a Maxwellian-like shape at low energy and thus grossly satisfy the collision operator at low energy in the way that the exponential atmosphere does exactly? The prototype distribution considered for the FIPH approach is the generalized Lorentzian or kappa distribution with characteristic speed w_{c_0}:

$$f_{\kappa_0}(N_0, w_{c_0}, \kappa_0, v, x_0) = \frac{N_0 A_{\kappa_0}}{\Gamma(1/2) w_{c_0}} \left(1 + \frac{v^2}{\kappa_0 w_{c_0}^2}\right)^{-(\kappa_0+1)}, \tag{7a}$$

which, after traversing a decelerating potential, becomes

$$f_{\kappa_0}(N_0, w_{c_0}, \kappa_0, v, x) = \left[1 + \frac{v_\phi^2(x)}{\kappa_0 w_{c_0}^2}\right]^{-(\kappa_0+1)} \times \frac{N_0 A_\kappa}{\Gamma(1/2) w_{c_0}} \left(1 + \frac{v^2}{\kappa_0 w_{c_0}^2 + v_\phi^2(x)}\right)^{-(\kappa_0+1)} \tag{7b}$$

$$= \left[1 + \frac{v_\phi^2(x)}{\kappa_0 w_{c_0}^2}\right]^{-(\kappa_0+1)} \times f_{\kappa_0}\left(N_0, w_{c_0}\left[1 + \frac{v_\phi^2(x)}{\kappa_0 w_{c_0}^2}\right]^{1/2}, \kappa_0, v, x_0\right). \tag{7c}$$

Although equation (7b) does not have the velocity-space congruence possessed by the EA solution of equation (5c), it does have a *self-similarity* property (eq. [7c]); an additional property is that the configuration and velocity space are no longer separable as they were in the exponential atmosphere. This latter property allows it to describe temperature variations while remaining consistent with the $Df_\kappa/Dt = 0$ requirement at high energy that is referred to above. The property of velocity space self-similarity and the structure of the function itself demonstrates that

$$f_\kappa(v, x) \simeq B(v_\phi(x), \kappa_0) \exp\left[-\frac{(\kappa_0 + 1)v^2}{\kappa w_{c_0}^2 + v_\phi^2(x)}\right]; \quad v^2 < 3\left(w_{c_0}^2 + \frac{v_\phi^2}{\kappa}\right). \tag{7d}$$

Thus, at low energies f_κ is very nearly a Maxwellian and thus nearly a solution of the scattering operator as desired by the FIPH approach. By construction at high energies, where collisions are unimportant, f_κ is an exact solution of $Df_\kappa/Dt = 0$ and there will be no corrections with increasing speed from "free streaming" to the lowest order distribution function. At high speeds compared with $\kappa^{1/2} w_c$, f_κ goes smoothly over into an inverse power law in velocity, resembling the ubiquitous suprathermal tails of *in situ* measurements.

Therefore, the FIPH approach does *not* really ignore the role of collisions. The Hybrid approach may be suitable for the approximate discussion of fully ionized stellar atmospheres (cf. Paper II), since it admits solutions for astrophysical plasmas that are non-Maxwellian, charge-neutral, and thermally inhomogeneous ($\partial T/\partial x \neq 0$) in the lowest order, while remaining self-similar to a Maxwellian at low energies.

The present paper takes a new look at the FIP closure problem by examining the moments of "restricted free-streaming" solutions of $Df_\kappa^{(0)}/Dt = 0$ for different boundary κ's to illustrate what kind of closure relations are induced in lowest order by conservative forces. This approach is useful for two classes of problems: first, the interaction of plasmas with extremely localized potentials where all species at all energies are collisionless, such as at a collisionless shock of MHD discontinuities (Vlasov); and, second, the interaction in a decelerating force field in a region that has a thickness L larger than the thermal mean free path (Hybrid).

Some of the effects recovered by this kinetic approach will be familiar, but they are presented for completeness to establish contact with more familiar results from macroscopic equations such as adiabatic compression and cooling of supersonic flows, and the well-known invariance of a Maxwellian temperature when interacting with a decelerating force. The sensitivity of the isothermal exponential atmosphere to the Maxwellian boundary condition leads to the exploration of new effects with potentially interesting astrophysical consequences when $\kappa \neq \infty$. These effects are developed graphically in § 3, in preparation for the quantitative work of § 4 and Paper II.

Velocity filtration is the most important new effect in the presence of an attractive potential: the plasma temperature can *reversibly* increase while the density decreases without any deposition of energy! This effect can occur when collisions have been "finessed" by the boundary condition choice of distributions that are quasi-Maxwellian at low energies and overpopulated at suprathermal energies relative to a Maxwellian of equivalent density and pressure. The resulting anti-correlation of temperature and density is unknown in

collisional gasdynamics; it is graphically shown to be a *general* property of suprathermal distributions regardless of whether or not a closed-form equation of state is possible. The Hybrid problem illustrates that velocity filtration can lead in the presence of a κ nonthermal boundary distribution function to a polytrope equation of state, but with $\gamma < 1$.

A general prescription is developed to predict the sign of the changes of the temperature of the gas as determined by the Mach number of the flow, the attractive and repulsive nature of the potential, and the collisionality of the gas. Because knowledge of the potentials that are important in an astrophysical system is usually much more accessible than a defensible closure approximation, such an investigation may be of use in diagnosing remote astrophysical plasmas.

3. QUALITATIVE SOLUTIONS TO SHOW EFFECTS OF POTENTIALS

The conserved quantities of the collisionless Boltzmann or Vlasov equation will guide the subsequent discussion. Conservation of energy for a one-dimensional phase space implies the spatial conservation of the energy flux, F_{iE}, for the ith species of temperature T_i; bulk speed U_i, density N_i, heat flux q_i, mass m_i, and conserved mass flux $F_{im} \equiv N_i m_i U_i$:

$$\left(\frac{1}{2} F_{im} U_i^2 + \frac{3}{2}\frac{F_{im} k T_i}{m_i} + \frac{F_{im}\psi_i}{m_i} + q_i\right) = F_{iE} . \tag{8}$$

The conservative body forces per unit mass density on the ith species of the gas are determined from $-\nabla\psi$. When the conserved mass flux, F_{im}, does not vanish, equation (8) may be factored, yielding the generalized Bernoulli constant E_i. Independent of the spatial structure of the equivalent potential ψ_i, E_i provides a general constraint on the interchanges in flowing gases of directed, internal, potential, and conduction "energies" per particle, viz.,

$$\left(\frac{1}{2} U_i^2 + \frac{3}{2}\frac{kT_i}{m_i} + \frac{2\psi_i}{m_i} + \frac{q_i}{m_i N_i U_i}\right) \equiv E_i = \frac{F_{iE}}{F_{im}} . \tag{9}$$

A one-dimensional phase space is examined in detail below because of its mathematical simplicity. Equations (8) and (9) are generalized to encompass a three-dimensional phase space and the magnetic field in Paper II.

As an initial example, a supersonic Maxwellian velocity distribution (illustrated in Fig. 2*b*) has been chosen as the boundary condition to interact with a reversible potential. In the limit of no collisions the evolution of the Vlasov equation becomes a simple form of Liouville's theorem, with the phase-space density being conserved while following the velocity space evolution of f at each v. By simple conservation of energy, this nonlinear prescription is

$$v'(\epsilon, x') = \frac{|v(x)|}{v(x)} [v^2(x) + \epsilon v_\Psi^2]^{1/2} , \tag{10a}$$

$$v_\Psi^2 \equiv \frac{2|\psi(x) - \psi(x')|}{m} , \tag{10b}$$

$$g(v'(x')) = f(v(x)) , \tag{10c}$$

where the $\epsilon = \pm 1$ branches in the mapping between x and x' apply to repulsive ($\epsilon > 0$) and attractive ($\epsilon < 0$) potentials, respectively. The deformation of the velocity distribution under equation (10c) transforms the supersonic Maxwellian distribution of Figure 2*b* into the heavy, continuous asymmetric curves in Figures 2*a* and 2*c* for the repulsive and attractive situations, respectively. The parameters of Figure 2*b* reflect Mach 12.5 flow; for the mapping illustrated in Figures 2*a* and 2*c* the ratio of v_Ψ to the bulk speed U is arbitrarily chosen to be $v_\Psi/U = 21/25$.

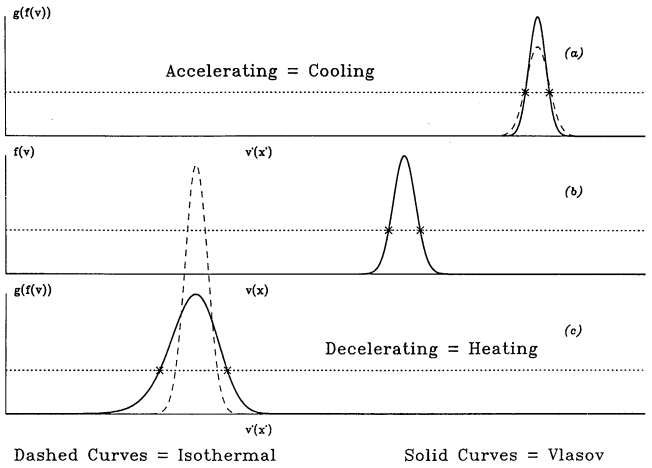

FIG. 2.—Supersonic regimes. Qualitative one-dimensional solution supersonic Maxwellian boundary condition: (*a*) repulsive potential; (*b*) boundary condition; (*c*) attractive potential. The horizontal axis is the particle's velocity.

The heavy curve in Figure 2*a* illustrates that the *spread* of the initial distribution of Figure 2*b* has been reduced by the accelerating force; this effect accompanies the dominant acceleration of the distribution as a whole, evidenced by the shifted peak of the solid curve distribution in Figure 2*a*. The widths at the $1/e$ level of the distributions in all three panels, indicated by crosses, reveal that the full width at $1/e$ of the distribution (and hence its dispersion) is indeed smaller in Figure 2*a* relative to that in Figure 2*b*. Kinetically, the distribution of Figure 2*a* is "cooler" than that in Figure 2*b*; spectroscopically, the thermal broadening of Figure 2*a* will be less than that in Figure 2*b*. Conversely, the same graphical procedure of the above mapping with the negative sign (same size v_Ψ as in the attractive mapping from Fig. 2*b* to Fig. 2*a*) yields the "heated" broadened distribution of Figure 2*c*. In addition to the broadening of the distribution and its downshift in mean speed, the heavy curve of Figure 1*c* clearly demonstrates that the mapped distribution developes a skew or heat flux in the bulk speed frame that the symmetric, supersonic Maxwellian distribution of Figure 2*b* does not possess. (A similar skewing occurs in Fig. 2*a* but is more difficult to perceive in the contracting width of the distribution.) The supersonic distributions of Figure 2 are deformed under the conservation of both equation (8) and equation (9); visually *all* the terms in equation (9) change while traversing the potential: the bulk speed/centroid increases (decreases), the temperature/dispersion decreases (increases), the potential energy decreases (increases), and the signed heat flux/skew decreases (increases) in size in Figure 2*a* (2*c*).

The comparison of e^{-1} widths in Figure 2 emphasizes the visual, rather than the quantitative, aspects of the "heating" and "cooling." Detailed calculations presented below (§ 5) confirm that the moment fluid temperature in supersonic flows (as the appropriate moment in the comoving frame) does indeed systematically decrease for accelerating potentials and increase for decelerating potentials. Such behavior is also

expected in supersonic flow based on the mathematics of the fluid moment equations. The present approach retrieves this result from the kinetic perspective and illustrates the role of the force in the temperature change. The macroscopic fluid equations predict the result of adiabaticity without commenting on how it happens. One immediate clarification is that the adiabatic approximation is at best a supersonic closure concept.

The dashed traces on Figures 2*a* and 2*c* indicate the Maxwellian distributions ($q = 0$) with temperature equal to that of the boundary distribution assumed in Figure 2*b*, but with a density modified as necessary to conserve mass flux and to conserve the energy flux of the distribution in Figure 2*b*. The Vlasov solutions rigorously conserve energy and mass fluxes without any additional assumption about the statistical mechanics of the gas. The dashed and dotted curves are actually quite different, given the linear scales of the ordinate. These dashed curves are the lowest order distribution of polytropic closure with $\gamma = 1$. A significant difference exists between the Vlasov solution and the homogeneous isothermal Maxwellian, making a perturbative set of corrections unlikely. The supersonic character of the initial data rules out the direct relevance of the SB approach. These figures apply equally well to the same potential jump distributed over 10 or a million kilometers, provided that the potential profile remains monotonic.

Finally, the nonzero spread of the initial distribution controls the deformation by the potential in a crucial way: if the distribution function were a delta function, no deformation of f would take place; see § 4 below. In this regime no difference would exist between a probability distribution function and a particle with no internal degrees of freedom; the temperature would be zero before and after traversing the potential, and bulk energy would be the sole reservoir for exchanges with the potential energy reservoir (cf. eq. [9]).

The supersonic Vlasov behavior of Figure 2 is a special case of the more complicated interrelationships possible between T and N. Figure 3 concerns the graphical analysis of the stationary Maxwellian boundary condition under repulsive and attractive potentials. The format of Figure 3 differs from that of Figure 2 in using a semilogarithmic format, $\ln f$ versus *local* kinetic energy KE(x'). The retarding force causes the probability distribution in this coordinate system to shift rigidly in the energy space. The horizontal axis retains (for convenience) the sign of the velocity of the characteristic involved. The triangular distribution of Figure 3b is a Maxwellian at rest, with its moment temperature, T_0, synonymous with that determined by the operation $-1/kT(\xi) = d\ln f(\xi)/d\,\mathrm{KE}(\xi)$, independent of ξ. The restatement of equations (10b) and (10c) in terms of the kinetic energy KE at x and KE′ at x', separated by the potential difference of $\epsilon|\Delta\psi|$, is given by

$$\mathrm{KE}'(x') = \mathrm{KE}(x) + \epsilon|\Delta\psi| \quad \text{for all KE}' > 0\,, \qquad (10b')$$

$$g(\mathrm{KE}', x') = f(\mathrm{KE}, x)\,. \qquad (10c')$$

Equivalently, the Vlasov solution $g(x')$ reflects a rigid translation in energy of $f(x)$ *for those trajectories that are accessible from* x *to* x'. The particles in regions A and B in Figure 3*b* are not found at x' in Figure 3*c* because they do not satisfy equation (10*b*′), but they are found in the repulsive potential in Figure 3*a*; *this process of exclusion* of the lower kinetic energy particles of the phase space *in an attractive potential described by equation* (*10*) *has been given the name "velocity space filtration."*

The filtration process reflects nothing more than the synthesis of conservation of energy, particle by particle. Those trajectories of sufficient kinetic energy KE to have nonnegative kinetic energy KE′ at x' rigidly "carry" (by the method of characteristics) their portion of f at x to the new kinetic energy at x' according to equation (10*c*′). The points of immediate interest in Figure 3*c* are that *both* (1) the density and (2) the pressure of the gas at x' are reduced by the interaction with the attractive potential; however, the logarithmic derivative of the distribution g at all ξ, $d\ln g/d\,\mathrm{KE}'|_\xi = -1/kT'(\xi)$, equals $d\ln f/d\,\mathrm{KE} = -1/kT_0$, because the slopes of f in regions C and D in the Maxwellian of Figure 3*b* are the same as they are in regions A and B. For this boundary condition, excluding particles from reaching x' in the attractive potential does not change the dispersion of $g(v, x')$ or, therefore, the temperature of the gas (cf. § 5). This effect is well known and underlies the property of the exponential atmosphere (Maxwell 1873; Boltzmann 1875). No new effects or hints of potential velocity space instabilities occur in a three-dimensional space.

The repulsive potential case of Figure 3*a* is even more complicated. If the boundary data have no net momentum and represent an even boundary function of v, a steady state solution of Vlasov has two separate energized peaks moving in opposite directions at x', for $\epsilon = 1$. Such a distribution is two-stream–unstable. The actual instability of such distributions depends on the response of the part of the distribution function perpendicular to the local magnetic field. The isomagnetic acceleration depicted in Figure 3*a* is indeed two-stream–unstable. If this accelerating force is accompanied by an increasing magnetic intensity, as in a fast-mode sock (cf. Scudder et al. 1986a, b, c), a velocity space with an elliptical void is formed that is not two-stream–unstable; for a decreasing field strength as across a slow mode shock, the field behavior may exacerbate the two-stream instability. Whether such interactions can be distilled into a local closure law is not clear.

A generic nonthermal boundary distribution has the property that $(-d\ln f/d\,\mathrm{KE})^{-1}$ is an increasing function of kinetic energy as illustrated in Figure 4*b*. Nonthermal distributions

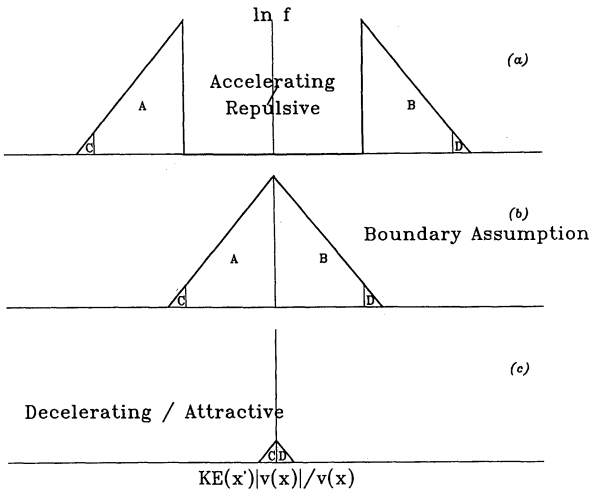

FIG. 3.—Degeneracy of Maxwellian. Qualitative one-dimensional solution for Maxwellian at rest boundary condition. The horizontal axis is the particle's local kinetic energy with the sign of the velocity of the characteristic's location in the boundary velocity space, viz., $\mathrm{KE}(x')\,|\,v(x)\,|/v(x)$: (*a*) repulsive potential at x; (*b*) boundary condition at x; (*c*) attractive potential at x.

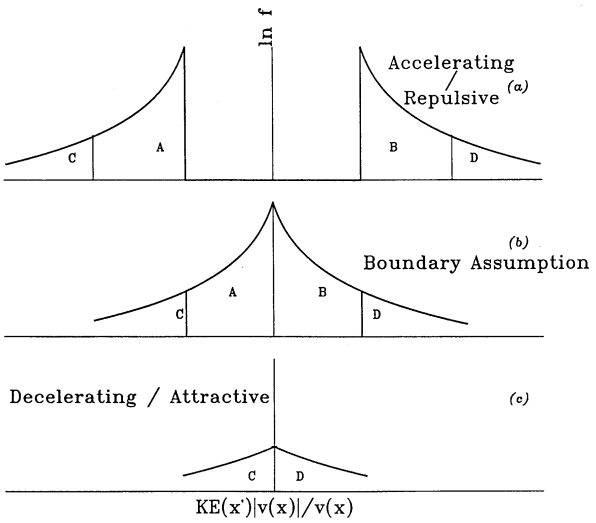

FIG. 4.—General subsonic case, nonthermal boundary assumption. Qualitative one-dimensional solution suprathermal distribution at rest: modifications (*a*) at x' under acceleration; (*b*) at boundary condition at $x = 0$; (*c*) at x' under deceleration. The horizontal axis is the same as in Fig. 3.

are invariably observed in astrophysical plasmas where *in situ* measurements of high quality have been made (Vasyliunas 1968; Montgomery et al. 1968; Ogilvie et al. 1971a, b; Montgomery 1972; Feldman et al. 1973; Ogilvie et al. 1974, 1977; Bridge et al. 1974; Feldman et al. 1975; Rosenbauer et al. 1976; Krimigis et al. 1981; Scudder, Sittler, & Bridge 1981; Sittler, Scudder, & Bridge 1981; Marsch & Goldstein 1983; Riehl & Hardy 1986; Christon et al. 1991). The "temperatures" at kinetic energy KE (defined as $k''T''_{\rm KE} \equiv (-d\ln f/d\,{\rm KE}'|_{\rm KE})^{-1}$ are invariably larger at the higher energies of the suprathermal tails than at the lower portion of the distribution function, except for examples of inelastic degradation by neutrals (Hartle et al. 1982) or dust (Sittler et al. 1981).

A graphical solution for a generic nonthermal boundary distribution interacting with an attractive potential is illustrated in Figure 4*c*. As in Figure 3*b*, particles from regions A and B of Figure 4*b* cannot be found at x' in Figure 4*c* because of the energetics of "filtration"; the resulting "filtered" distribution shown in Figure 4*c* at x' results from the rigid juxtaposition about the velocity space origin of the phase-space regions C and D of Figure 4*b*. This filtration process has clearly reduced the pressure *and* the density at x' relative to those at x; however, unlike the filtered Maxwellian case in Figure 3*c*, the dispersion of the distribution in Figure 4*c* which is synonymous with the kinetic temperature is clearly larger than that at x in Figure 4*b*. This example illustrates that $T(x')$ can vary *inversely* with the density; if a polytrope closure relation were possible, it would require $\gamma < 1$ to describe this behavior. *Any form of suprathermal tail in the boundary distribution function causes the anticorrelation between T and N illustrated here. Furthermore, the anticorrelation of T and N results from the reversible interaction with an attractive potential.*

Figure 4*a* shows the similar broadened "heating" effect of the repulsive potential on the nonthermal $f_{\rm boundary}$ that was seen in the interaction of the Maxwellian and the repulsive potential illustrated in Figure 3*a*.

Figures 3 and 4 pertain to boundary conditions that are perfectly symmetric in velocity space and have $F_{im} = F_{iE} = 0$; such a gas possesses only a global energy flux conservation law to constrain the possible effect of the potential on the temperature and heat flux. In this regime $u = q = F_E = 0$, and the changes in kT and ψ are only constrained by conservation of energy (cf. eqs [30a] and [30b] below) and the characteristics, since the conservation laws guarantee by symmetry that $q(x) = F_E = 0$ throughout.

4. MATHEMATICAL SOLUTIONS

To discuss a broader range of initial distributions, including the subsonic and transonic boundary condition flows, a more systematic mathematical discussion is now required. Four broad issues are involved: (1) the possible, astrophysically relevant boundary conditions worth examining: (2) the consistency required of the boundary data for a well-posed problem; (3) the role of nonlocality, and (4) the necessary ingredients for analytic closure.

Solutions of the collisionless Boltzmann equation must be functions solely of the conserved quantities of the system. Given this mathematical freedom, the initial conditions should have a physical connection to a system where the phase space is well known. For the case of the solar atmosphere the initial distribution function presumably has a single maximum in velocity space and a resemblance to a quasi-Maxwellian at least at low energies for some portion of the low-energy phase space; this is reasonable, since the plasma at the surface of the star was recently in a much more homogeneous and dense medium that could ensure that most of its form was Maxwellian and is consonant with the FIPH premises. For boundary conditions that are relevant for the ultimate solar wind expansion, these initial data should have a mass and a particle heat flux; for a closed coronal loop, generally this is not necessary.

The values of the initial/boundary distribution function are conserved along the characteristics in the absence of collisions. The topology of these paths is different for attractive and repulsive potentials. The types of solutions determine (*a*) whether the assumed boundary conditions are mathematically well posed, (*b*) whether simple closure relations are possible, and (*c*) the onset of nonlocality. These are now considered in turn.

A generic monotone repulsive potential [$\psi(x) = 0$] determines the spatial locations of the curves of constant total energy indicated in Figure 5; these curves are the characteristic curves of constant probability density; these, in turn, are the level surfaces of the Vlasov solution. The level values of the distribution are determined once the boundary function(s) is (are) prescribed. The $x = 0$ boundary distribution *can* be freely specified and still achieve a time-independent solution. Operationally this is clear, since no characteristic that crosses the left boundary at ($x = 0$, v_1) recrosses $x = 0$ at some other velocity v_2.

An attractive potential can "trap" a subset of characteristics that emanate from ($x = 0$, v) whenever these initial trajectories correspond to a total energy $E \leq \Delta\psi$, the barrier height between x and x'. Particles of such energy cannot energetically reach x' emanating from x. Whenever $E(x = 0) \leq \Delta\psi$, the $x = 0$ data cannot be independently chosen at the two oppositely directed velocities of the same energy within the trapped region along the same boundary. Since f is conserved along trajectories and $E(x, v)$ is quadratic in v at $x = 0$, this constraint translates to the requirement that $f(v, x)$ be an even function of v for $|v| < v_\Psi$, where $0.5mv_\Psi^2 \equiv e\Delta\psi$, the potential energy increase across the solution space of Figure 6.

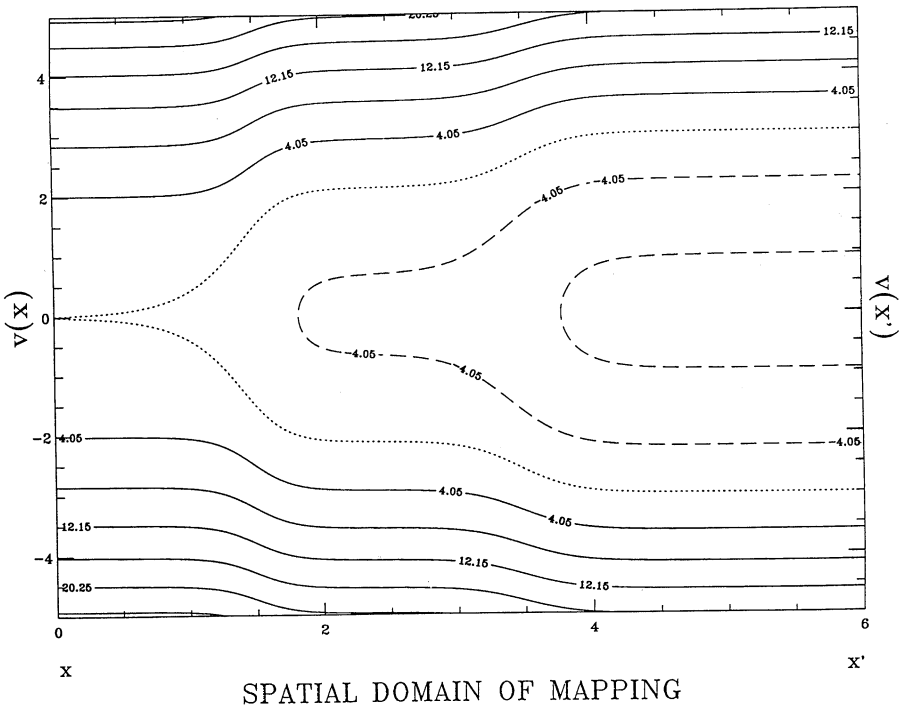

FIG. 5.—Accelerating potential's characteristics. *Solid* (*dashed*) *contours*: trajectories of positive (negative) total energy. Dotted contour is $E_{total} = 0$ trajectory. The zero of potential energy is at $x = 0$. Characteristics that cross $x = 6$ twice define the "trapped" portion of the boundary data.

The global character of steady state Vlasov solutions is most clearly seen by contrasting the interval of reentrant characteristic trajectories with the interval in velocity space where the $x = 0$ distribution is nonzero. When the boundary distribution chosen at $x = 0$ "straddles" $v_x = 0$, the constancy of f along the characteristics implies other boundary choices as well. Characteristics that traverse both spatial boundaries can potentially also contribute to the nonlocal character of the steady state solution. In a steady state there is no causality, just a consistency requirement. These "straddling" boundary conditions require two types of consistency: (*a*) implied sympathetic definition of boundary conditions on boundaries

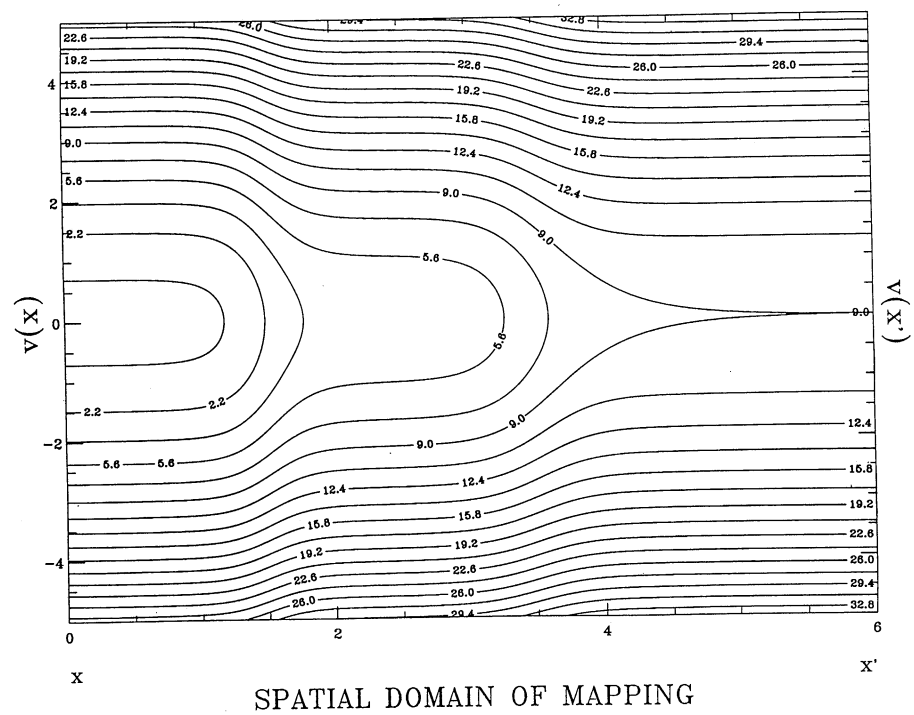

FIG. 6.—Decelerating potential's characteristics. The zero of potential energy is at $x = 0$. *Solid contours:* trajectories of positive total energy. Characteristics that cross $x = 0$ twice define the "trapped" portion of the boundary data at $x = 0$.

connected with characteristics that can happen for either attractive or repulsive potentials; and (*b*) prohibition of asymmetric choices of boundary conditions $f(v, x = 0)$ for those parts of $f(v, x = 0)$ where $|v| < v_\Psi$, as in the case of attractive potentials (cf. Fig. 6), or $f(v', x')$ for $|v'(x')| < v_\Psi$ for repulsive potentials (cf. Fig. 5). Both of these counterintuitive aspects result in a nonlocal, steady state solution that cannot be anticipated by following the Lagrangian evolution of a Vlasov fluid element as it would evolve with a time arrow.

For repulsive potentials the "flow" of information from the $x = 0$ boundary condition does not return. If the $x = 0$ boundary data for attractive potentials is only nonzero outside the "reentrant" characteristics of $E < 0$ (like the supersonic example of Fig. 2*b*), then it also will have the simplicity of hyperbolic partial differential equations, and the spatial distribution function in steady state will correspond to a gradual evolution in a "causal" way from the left boundary condition to the right. An alternative definition of nonlocality, then, would be the degree to which the initial data projects onto the "reentrant" characteristics and/or implicitly determine two spatially separated boundary conditions. At the macroscopic level, the circumstances of kinetic nonlocality are regimes of subsonic or transonic flow, with information (characteristics) flowing in directions different from the bulk velocity.

Analytical and numerical calculations will now be used to illustrate the interrelationships between macroscopic parameters induced by the Vlasov equation. The approach is to consider a one-dimensional phase space, and a monotonic potential profile, and to contrast the macroscopic moments on either side of the entire change in the potential; similar techniques are used in subsequent papers to explore the spatial variation of a given steady state solution as the spatial coordinate between boundaries is varied. The concepts and the effects of a full three-dimensional phase space including magnetic intensity variations in a nonmonotonic potential have been used and compared with observations elsewhere (Scudder 1987a, b, 1989, 1992a) and contain similar effects.

In view of the sensitivity of our graphical analysis of Figures 3 and 4 to the presence of suprathermal tails, a functional family of one-dimensional boundary velocity distribution functions has been selected that, while naturally containing suprathermal "tails" as in Figure 4, has a limiting case that is the Maxwell-Boltzmann distribution of Figure 3. As discussed above for the FIPH approach, a desirable feature for such a family of distributions is that it should resemble a Maxwellian at low energy in order to be consistent with the Hybrid approach outlined above. A simple distribution function family of this type, introduced by Olbert et al. (1968) and Olbert (1969) to organize early space probe data (Vasyliunas 1968), is called the kappa distribution, f_κ, after the parameter κ whose *inverse* indexes the degree of departure at suprathermal energies from a convected Maxwellian. The one-dimensional convecting kappa distribution is defined by the relation

$$f_\kappa(N, U, w_c, \kappa, v) = \frac{NA_\kappa}{\Gamma(1/2)w_c}\left[1 + \frac{(v - U)^2}{\kappa w_c^2}\right]^{-(\kappa+1)}, \quad (11a)$$

where w_c is a characteristic speed of the distribution, and U is a component of the bulk velocity. A_κ is a normalization constant of order unity defined in terms of the gamma function by the relation

$$A_\kappa = \frac{\Gamma(\kappa + 1)}{\kappa^{1/2}\Gamma(\kappa + 1/2)}. \quad (11b)$$

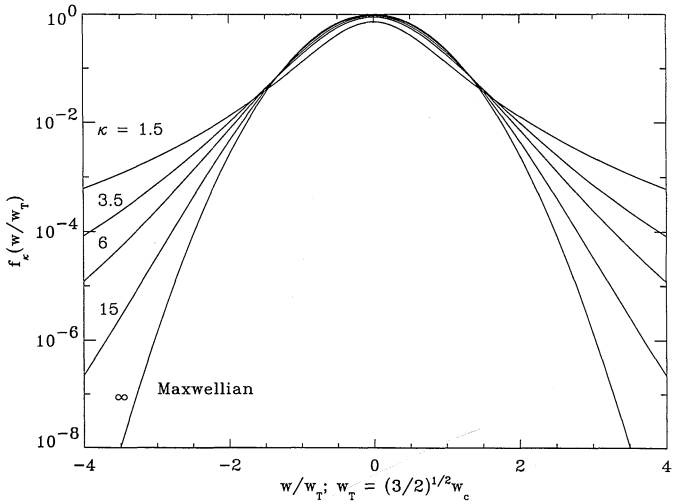

FIG. 7.—Internormalized kappa suprathermal family. Representative members of the generalized Lorentzian, or kappa, distribution family introduced by Olbert et al. (1968), Olbert (1969), chosen to model *in situ data* (e.g., Vasyliunas 1968; Owocki & Scudder 1983; Christon et al. 1991) with its ubiquitous inflation of the suprathermal tails at the expense of the thermal population; also shown is the limiting form when $\kappa \to \infty$, the Maxwell-Boltzmann distribution.

In the limit as κ goes to infinity, $f_\kappa \to f_M$, the well-known Maxwell-Boltzmann distribution, with temperature $kT_i = m_i w_c^2/2$ and bulk speed U. At low energies the κ distribution strongly resembles a Maxwellian whenever $|v - U|^2 < \kappa w_c^2$. Representative, normalized kappa distributions (including the Maxwellian limit) are depicted in Figure 7. Shown in the fluid rest frame, these curves illustrate the enhancement of suprathermal tails as κ becomes smaller, and the simultaneous reduction of $f_\kappa(v = 0)$ and growth of the *e*-folding width, so that the total number of particles in the different contrasted distributions remains the same.

The velocity space mapping of equation (10) dictates the size of the moments of the velocity distribution $g(v', x')$ at x': they are the density ($\lambda = 0$), the number flux ($\lambda = 1$), and the pressure ($\lambda = 2$), determined by the method of characteristics to be

$$\langle v^\lambda \rangle_\epsilon = \frac{N_0 w_c^\lambda A_\kappa}{\Gamma(1/2)} \int_{\Psi(1-\epsilon)/2}^{\infty} d\chi\, \chi(\chi^2 + \epsilon\Psi^2)^{(\lambda-1)/2} \times \left\{\left[1 + \frac{(\chi - \mu)^2}{\kappa}\right]^{-(\kappa+1)} + (-1)^\lambda \left[1 + \frac{(\chi + \mu)^2}{\kappa}\right]^{-(\kappa+1)}\right\}. \quad (12)$$

These fluid moments are functions of a dimensional and three dimensionless variables: the Mach number μ of the flow, defined as $\mu \equiv U/w_c$; the dimensionless positive speed equivalent of the potential energy shift, defined as $\Psi \equiv |v_\Psi|/w_c$; and the dimensionless kappa parameter, κ, which indexes the proximity of the boundary distribution at x to a drifting Maxwell-Boltzmann distribution.

Defining the moment variables at x' corresponding to density N, bulk speed U, and temperature T, we have

$$N(x') = N(N_0, w_c, \kappa, \mu, \epsilon\Psi, x') = \langle v'^0 \rangle, \quad (13)$$

$$U(x') = U(w_c, \kappa, \mu, \epsilon\Psi, x') = \frac{\langle v'^1 \rangle}{\langle v'^0 \rangle}, \quad (14)$$

$$\frac{2kT(x')}{m} = \frac{2kT(w_c, \kappa, \mu, \epsilon\Psi, x')}{m} = \frac{\langle v'^2 \rangle}{\langle v'^0 \rangle} - \left(\frac{\langle v'^1 \rangle}{\langle v'^0 \rangle}\right)^2, \quad (15)$$

where the correction term in equation (15) removes the dynamic pressure from $\langle v'^2 \rangle$ associated with the bulk flow.

By examining the fractional changes of these moment quantities with respect to their values for the distribution at x (where $\Psi = 0$), we can define three variables, $\{\eta, \Upsilon, \tau\}$, that only depend on the three dimensionless variables introduced above, $\{\kappa, \mu, \epsilon\Psi\}$, viz.:

$$\eta(\kappa, \mu, \epsilon\Psi, x') \equiv \frac{N(x') - N(x)}{N(x)}, \tag{16}$$

$$\Upsilon(\kappa, \mu, \epsilon\Psi, x') \equiv \frac{U(x') - U(x)}{U(x)}, \tag{17}$$

$$\tau(\kappa, \mu, \epsilon\Psi, x') \equiv \frac{T(x') - T(x)}{T(x)}. \tag{18}$$

In general, when a distribution with $\mu \neq 0$ is assumed for a boundary condition, the equilibrium solutions contain spatial variations in the presence of the potential as constrained by the Bernoulli constant E_1. When F_E does not vanish, this constrains the bulk speed, species temperature, and heat flux. In this paper the systematics of this interrelationship are demonstrated by contouring η, Υ, τ as functions of the initial parameters that characterized the initial state of the plasma: κ parameterizes the extent of departure from a local comoving Maxwellian, μ its Mach number, and $\epsilon\Psi$ the signed square root of the relative size of the potential energy change between the two locations under consideration in units of the initially prepared thermal energy; $\epsilon > 0$ corresponds to accelerating forces and $\epsilon < 0$ to decelerating ones.

An arbitrary boundary function assumption, $f_B(v)$, from equation (11a) will not be symmetric for $|v| < v_\Psi$ as required in the case of attractive potentials. To have an illustrative and nonunique but well-posed Vlasov problem, f_B is assigned the values of f_κ from equation (11a) for all $|v| \geq \Lambda(\epsilon) \equiv v_\Psi(1 - \epsilon)/2$, but $f_B = C$ for $|v| < \Lambda(\epsilon)$, where C is chosen so that $\langle f_B v \rangle / \langle f_B \rangle = \langle f_\kappa v \rangle / \langle f_\kappa \rangle$. This guarantees that the Mach number property that is used to organize the present discussion is preserved through the choice of C. It does, however, imply that the temperature and density of the boundary function are changed for each different v_Ψ assumed in the attractive portions of Figures 8–10 (cf. eqs. [16] and [18]). Accordingly, the temperature enhancements $T(\psi)/T(\psi = 0, \epsilon < 0)$ are reduced, because the reference $T(\psi = 0, \epsilon < 0)$ increases by this particular choice of the boundary function as the height of the repulsive barrier increases.

Figures 8a–8c illustrate the variations of τ, Υ, and η with w_c fixed, for a fixed kappa ($\kappa = 2$), for varying assumptions of (μ,

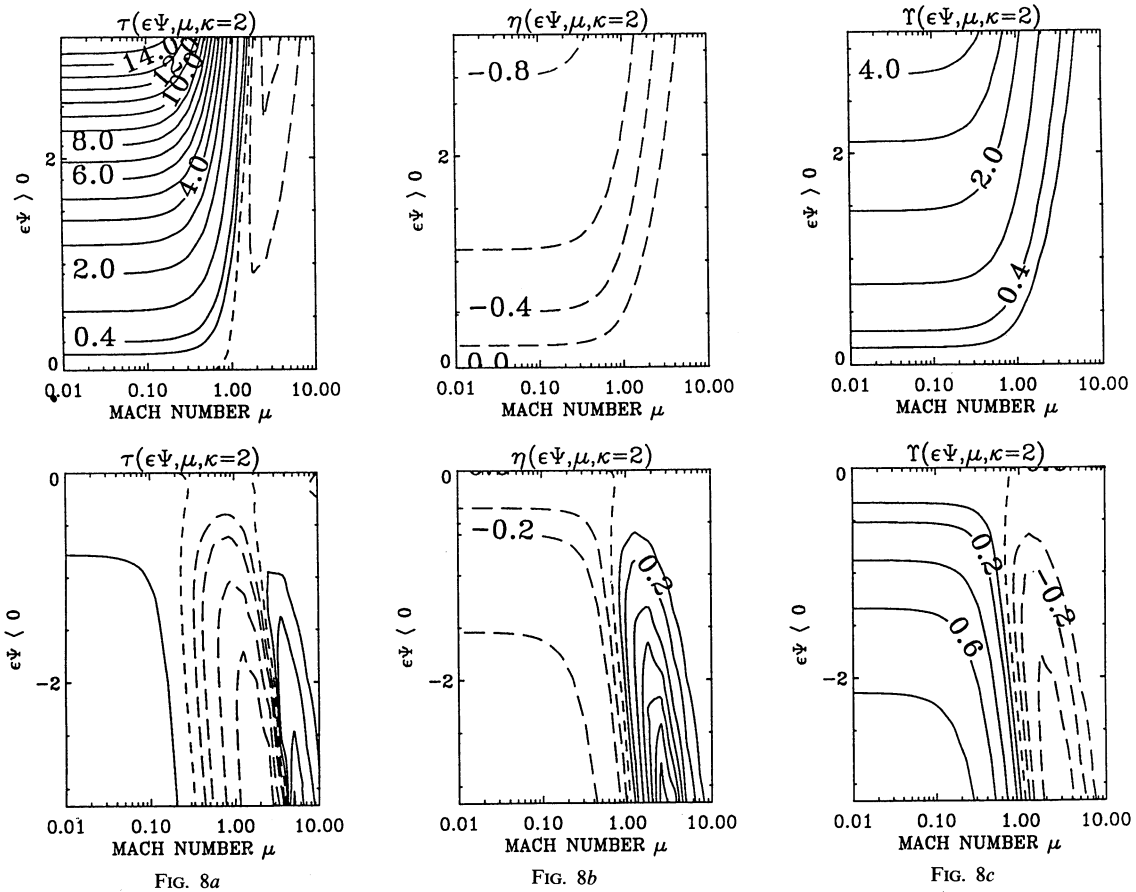

FIG. 8a FIG. 8b FIG. 8c

FIG. 8.—(*a*) τ-curves for repulsive ($\epsilon\Psi > 0$) and attractive ($\epsilon\Psi < 0$) potentials for a $\kappa = 2$ boundary distribution function. The horizontal axis is Mach number μ, and the vertical axis is $\epsilon v_\psi / w_c \equiv \epsilon\Psi$, whose square is proportional to the energy shift involved in the potential traversed. Contour levels in the upper subpanel, in increasing order, are (−0.4, −0.2, 0, 0.2, 0.4, 1, 2, 3, 4, 5, 6, 7, 8, 9, 10, 11, 12, 13, 14, 15). Those for the lower subpanel are (−0.6, −0.4, −0.2, −0.1, 0, 0.1, 0.2, 0.4, 0.6, 0.8). (*b*) η-curves for repulsive and attractive potentials for *a* $\kappa = 2$ boundary distribution function. The horizontal axis is μ; the vertical axis is $\epsilon\Psi$. Contour levels in the upper and lower subpanels are (−0.8, −0.6, −0.4, −0.2, 0) and (−0.4, −0.2, −0.1, 0, 0.1, 0.2, 0.4, 0.6, 0.8, 1.0, 1.2), respectively. (*c*) Υ-curves for repulsive and attractive potentials for a $\kappa = 2$ boundary distribution function. The horizontal axis is μ, the vertical axis $\epsilon\Psi$. Contour levels in upper and lower subpanels are (0, 0.2, 0.4, 1, 2, 3, 4) and (−0.4, −0.2, −0.1, 0, 0.1, 0.2, 0.4, 0.6, 0.8), respectively.

$\epsilon\Psi$). The upper panel corresponds to repulsive potentials and the lower panel to attractive ones. The dashed contours represent depressions, while solid isocontours denote ridges. Two simple regimes are clear in the τ topography in Figure 8*a*: (1) the very lowest ultra-subsonic ($\mu \simeq 0$) regime and (2) the extremely supersonic ($\mu \gg 1$) regime. Figure 8*a* quantitatively reinforces the qualitative impressions (cf. Figs. 3 and 2, respectively) of the heating and cooling induced by the action of these potentials. *In the extreme subsonic regime both attractive and repulsive potentials increase the temperature of the gas.* In the extreme supersonic regime, repulsive potentials cool the gas and attractive ones warm it. The transonic $\mu \simeq 1$ regime is more complicated, with a broad regime in the attractive potentials that yields cooling centered along the line $\mu = -\Psi$ supplanted by heating for $|\epsilon\Psi| \ll \mu$, where attractive potentials again heat the gas. A narrow regime of cooling followed by heating occurs for slightly supersonic flows ($\mu \simeq 1$) and repulsive potentials for larger attractive potential changes. The trends of heating and cooling for transonic distributions cannot be generalized, since the results are extremely dependent on the model symmetrization of the f_B for $E < \Delta\psi$.

Figure 9*a* illustrates similar relationships as f_B more nearly approximates a Maxwell-Boltzmann distribution. This figure reinforces the qualitative impressions of Figures 3 and 4. The numerical integrations of equation (7) have recovered the nearly isothermal response in the attractive potential of nearly Maxwellian distributions. In the supersonic limit Figure 9*a* illustrates the heating of the attractive potentials and the cooling of the repulsive potentials discussed qualitatively in Figures 3*a*–3*c*. Also indicated is the general heating of supersonic distribution in attractive potentials.

Figures 8*b* and 9*b* and 8*c* and 9*c* show in the same format the changes implied by the Vlasov equation for the density and bulk speed. The density and speed changes in Figures 8*b* and 8*c* and Figures 9*b* and 9*c* are anticorrelated as required for mass conservation. With increasingly supersonic boundary conditions the gas behaves more like a macroparticle; these calculations increasingly recover the property that repulsive potentials speed up and the attractive potentials slow down the gas, as graphically illustrated in Figures 2*a* and 2*c*.

Perhaps against one's intuition, opposite forces always cause ultra-subsonic distributions to speed up and their densities to reduce (cf. Figs. 8*c* and 9*c*). This is less surprising in the repulsive potential than in the attractive one. First, in the attractive potential, those particles that can overcome the barrier have more kinetic energy on average than those that cannot; second, because not all particles can get over the barrier, and as mass flux must be conserved, the speed must go up so that

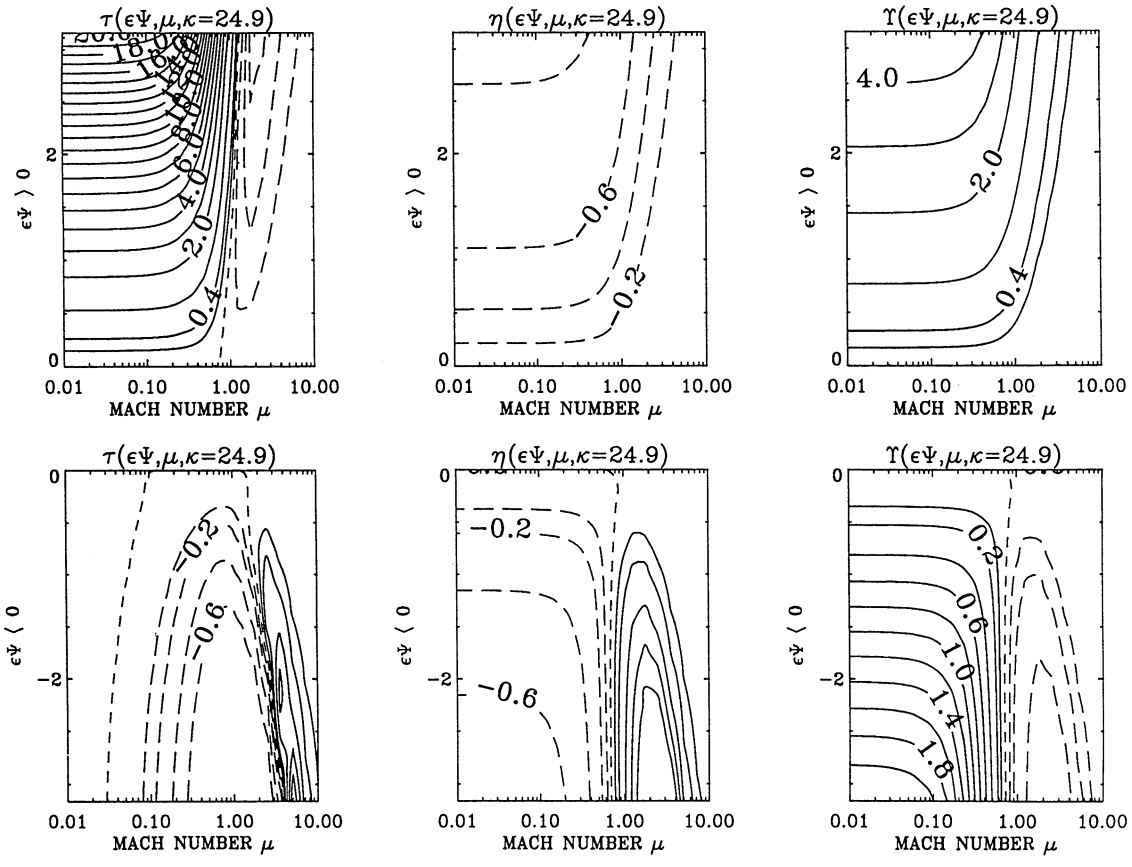

FIG. 9*a* FIG. 9*b* FIG. 9*c*

FIG. 9.—(*a*) τ-curves for repulsive and attractive potentials for a $\kappa = 24.9$ boundary distribution function. The horizontal axis is μ, the vertical axis $\epsilon\Psi$. Contour levels in upper the lower subpanels are (−0.6, −0.4, −0.2, 0, 0.2, 0.4, 1, 2, 3, 4, 5, 6, 7, 8, 9, 10, 11, 12, 13, 14, 15, 16, 17, 18, 19, 20) and (−0.6, −0.4, −0.2, −0.1, 0, 0.1, 0.2, 0.4, 0.6), respectively. (*b*) η-curves for repulsive and attractive potentials for a $\kappa = 24.9$ boundary distribution function. The horizontal axis is μ, the vertical axis $\epsilon\Psi$. Contour levels in upper and lower subpanels are (−0.8, −0.6, −0.4, −0.2, 0) and (−0.6, −0.4, −0.2, −0.1, 0, 0.1, 0.2, 0.4, 0.6, 0.8), respectively. (*c*) Υ-curves for repulsive and attractive potentials for a $\kappa = 24.9$ boundary distribution function. The horizontal axis is μ, the vertical axis $\epsilon\Psi$. Contour levels in upper and lower subpanels are (0, 0.2, 0.4, 1, 2, 3, 4) and (−0.4, −0.2, −0.1, 0, 0.1, 0.2, 0.4, 0.6, 0.8, 1.0, 1.2, 1.4, 1.6, 1.8, 2.0), respectively.

the smaller number of particles can carry the invariant mass flux assumed to exist in the boundary condition. *The filtration by number* in the attractive case *is the kinetic reason for the subsonic plasma to accelerate if it has any momentum at all at its inner boundary.*

5. ANALYTICAL CLOSURE APPROXIMATIONS

Several important closure relations can be obtained analytically and compared with the rigorous, corresponding calculations using the Vlasov mapping of the moments of equation (12) in three limiting regimes of practical astrophysical importance: (1) the ultra-supersonic regime for all repulsive potentials, (2) the ultra-supersonic regime for attractive potentials with $v_\Psi \ll U$, and (3) the ultra-subsonic regime for attractive potentials. These syntheses are possible because the variation of the size of the potential along the fluid streamlines does not *require* a boundary function change in the trapped region, $|v| \leq v_\Psi$, in order that the Vlasov problem be well posed.

5.1. *Supersonic Regime*

Referring back to Figure 2, we can estimate the change in the half-width of the distributions under the nonlinear mapping of equation (10). The particles at the $1/e$ points of the original beam have the velocities $v_\pm \equiv U \pm w$. Under the mapping of equation (10) they (and hence the e-folding points on the transformed f) will be found at new locations in velocity space given by

$$v'_\pm \equiv [(U \pm w)^2 + \epsilon v_\Psi^2]^{1/2} . \tag{19}$$

In the ultra-supersonic limit ($U \gg w$) the velocity space half-width of the modified distribution is approxmately $w' \equiv 0.5(v'_+ - v'_-)$ and the new bulk speed is $U' \simeq 0.5(v'_+ + v'_-)$. In this approximation U' and w' satisfy the identity

$$w'U' = wU , \tag{20a}$$

and may be estimated as

$$U'(\epsilon) \simeq (U^2 + w^2 + \epsilon v_\Psi^2)^{1/2}\left(1 + \frac{3}{4\mu^2}\right), \tag{20b}$$

$$w'(\epsilon) \simeq w\frac{U}{(U^2 + w^2 + \epsilon v_\Psi^2)^{1/2}}\left(1 - \frac{3}{4\mu^2}\right). \tag{20c}$$

In equation (20) μ is the species Mach number, $\mu = U/w$. Equation (20c) confirms the impression that if the initial distribution had no thermal half-width, then the accelerated one has no thermal width. Conversely, the force changes the temperature across a potential by dispersing or focusing the thermal width of the initial distribution (because of the nonlinearity of the basic transformation of eq. [10a]). These results allow an estimate of the fractional moment temperature change of equation (18):

$$\tau(\epsilon, \text{ ultra-supersonic regime}) \simeq \frac{-\epsilon v_\Psi^2 - w^2}{U^2 + w^2 + \epsilon v_\Psi^2} . \tag{21}$$

Equation (21) shows that the plasma cools for any accelerating ($\epsilon = 1$) potential and should be heated when the beam is strongly decelerated ($\epsilon = -1$, $v_\Psi^2 \gg w^2$), as qualitatively demonstrated in Figure 2. Some residual cooling is projected by equation (21) for weakly attractive potentials when $\mu \gg 1$ and $v_\Psi^2 < w^2$, as has already been demonstrated in Figures 8*a* and 9*a* near Mach number 10.

The ratio of the new to the old temperatures via equation (20a) is approximately given by

$$\frac{T_1(\epsilon v_\Psi^2)}{T_0} \simeq \frac{U_0^2}{U_1^2} , \tag{22}$$

conservation of mass flux dictates that $n_0 U_0 \equiv n_1 U_1$. Accordingly, equation (22) can now be rewritten in approximate polytropic form:

$$\frac{P_1(U_0 \gg w_0, \epsilon v_\Psi^2)}{P_0} \simeq \left(\frac{n_1}{n_0}\right)^3 , \tag{23a}$$

with index $\gamma \simeq 3$, corresponding to a one-dimensional adiabatic compression in the direction of acceleration. A slightly more accurate estimate of the polytrope may be had by estimating the various integrals involved via steepest descent (without making the approximations of eqs. [19]–[22]). In this case the polytrope exponent may be determined by $\gamma = (d \log T/d\psi)/(d \log n/d\Psi) + 1$ with the asymptotic, slightly superadiabatic result

$$\gamma(\kappa = \infty, \mu \gg 1) \simeq 3 + 2/\mu^2 . \tag{23b}$$

To show the fidelity of this approximation, Figure 10 illustrates the comparison between the improved theoretical value of equation (23b) and the slope of log P versus log n induced by different potentials ψ as κ increases, as determined by the numerical integration of moments (eq. [12]) in this supersonic regime. Each symbol plotted is the result for a given κ_0 of a slope determined by the method of linear least squares of the joint variation of log $P(\kappa_0, \psi)$ versus log $n(\kappa_0, \psi)$, while the solid line represents the expected asymptotic ($\kappa \to \infty$) polytrope exponent of equation (23b) for the present case of $\mu = 12.5$. The numerically determined estimates for $\gamma(\kappa, \mu = 12.5)$ are clearly shown to approach asymptotically the limiting form given in equation (23b) as κ increases.

A visual comparison of the approximation of equation (23b) in terms of the implied velocity distributions is given in Figure 11, in the same format as Figure 2. The solid curve is the streamed Vlasov solutions, while the dashed curve represents the Maxwellian approximation with density and temperature

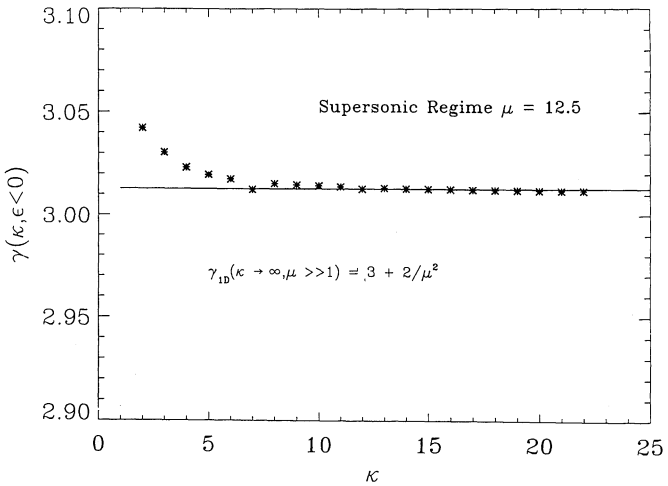

FIG. 10.—Polytrope verification. Comparison of theoretical supersonic polytrope constant from eq. (23b) with that determined numerically from $(d \log P/d\psi)/(d \log n/d\psi)$.

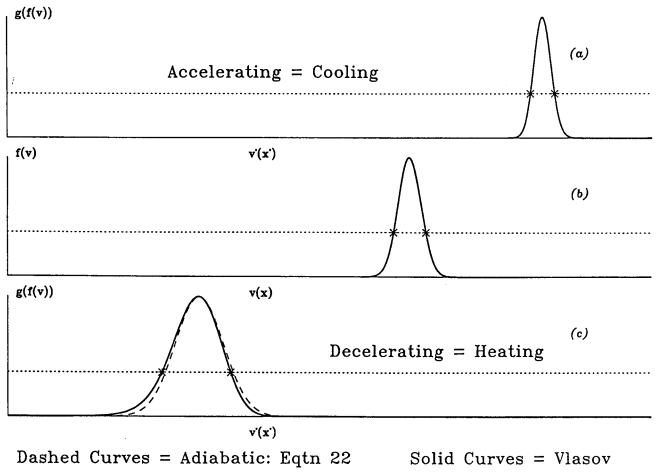

FIG. 11.—Supersonic regime. Comparison of Vlasov solution (*solid trace*) with adiabatic approximation to $f(v')$ given by eq. (24a, b).

dictated by equation (23b) at the accelerated bulk speed, viz.,

$$f_{\text{adiabatic}}(\epsilon, v'(x')) = \frac{n_0(x)\Sigma(x')}{\Gamma(1/2)[T_0(x)]^{1/2}} \times \exp\left\{-\frac{m[v'(x,\epsilon) - U'(x')]^2}{kT_1(\epsilon, x')}\right\}, \quad (24a)$$

where

$$\Sigma(x') \equiv \left[\frac{n'(x')}{n_0(x)}\right]^{-(1/\mu^2)} . \quad (24b)$$

Clearly this agreement is excellent and a perceptible improvement over the dashed isothermal approximation to the same Vlasov solution illustrated in Figure 2.

The supersonic beam's response shows clearly and simply that a potential can modify the temperature of the gas *in addition* to the intuitively expected modification of the bulk speed. The semiquantitative analysis and numerical work of the previous paragraphs establishes that the reversible interaction with a potential in the supersonic regime is approximated by, but deviates slightly from, one-dimensional adiabatic behavior.

5.1.1. *Ultra-subsonic Maxwellian Boundary Condition*

Figure 3 illustrated that the temperature of a Maxwellian collisionless gas initially at rest does not vary in space in the presence of an attractive potential. Such a thermal behavior has a simple isothermal closure relation, namely,

$$\frac{P_1(x', \epsilon = -1, f_M)}{P_0(x)} = \frac{n_1(x')}{n_0(x)} ; \quad (25)$$

equivalently, the polytrope exponent γ in this case is $\gamma(\mu = 0, \epsilon = -1, \text{Maxwellian}) = 1$, yielding an isothermal equation of state.

This same result is recovered analytically starting from equations (12), (13), and (15). With no bulk speed the temperature of the gas is proportional to the following expression:

$$\frac{\langle v'(x')^2\rangle}{\langle 1(x')\rangle} \equiv \int_0^\infty dv'\, v'^2 g(v'^2, x') \Big/ \int_0^\infty dv'\, g(v'^2, x') . \quad (26)$$

Using Liouville's theorem in the form $f(v^2, x) = g(v'^2, x')$, transforming the integrands in equation (26) into integrals over the phase space at x, exploiting equation (5c) and the definition of Ψ below equation (12), one can rewrite the quantity in equation (26) as

$$\frac{\langle v'(x')^2\rangle}{\langle 1(x')\rangle} \equiv \left[\exp(-\Psi^2)\int_0^\infty dv\, v^2 f(v^2, x)\right] \Big/ \left[\exp(-\Psi^2)\int_0^\infty dv f(v^2, x)\right] \quad (27a)$$

$$= \frac{\langle v(x)^2\rangle}{\langle 1(x)\rangle} . \quad (27b)$$

It follows that $\gamma = 1$. Of interest in this derivation is the reduction of pressure (numerator of eq. [27a]) and density (denominator eq. [27a]) by the *same* (Boltzmann) factor that leaves the temperature unmodified. The Gaussian transformation property (5c) played a pivotal role in deriving the isothermal equation of state implied by equation (27b).

5.1.2. *Ultrasubsonic Nonthermal Boundary Condition*

The schematic presentation of Figure 4 demonstrates that *the suprathermal tail is the essential aspect of the filtration heating effect*; hence, using a representative model for a distribution function that is in this class should yield results that are similar to any distribution that has a suprathermal tail. Fortunately, the behavior of a prototype nonthermal distribution can be determined analytically using the κ family of Figure 7. The equation of state in this particular case is polytropic, but of a type never used before in the theory of gases: one with the polytrope exponent less than unity for any finite κ. While this unusual polytrope relation is peculiar to this chosen boundary condition, the graphical example of Figure 4 illustrates that the *pressure will generally go down more slowly than the density for any suprathermal boundary distribution*, in much the same way as it does for a polytrope with $\gamma < 1$. *Thus the temperature-density anticorrelation is expected for any nonthermal distribution in an attractive potential whether a polytrope relation with $\gamma < 1$ can be proved or not.*

It follows from equation (11a) with $U = 0$ that

$$P(x', \epsilon = -1, f_\kappa) = P(x)\left(\frac{\kappa w_c^2 + v_\Psi^2}{\kappa w_c^2}\right)^{-\kappa+1/2} , \quad (28)$$

$$N(x', \psi, \epsilon = -1, f_\kappa) = N(x)\left(\frac{\kappa w_c^2 + v_\Psi^2}{\kappa w_c^2}\right)^{-\kappa-1/2} . \quad (29)$$

The ratio of equations (28) and (29) yields the variation of the temperature profile as a function of the potential barrier traversed:

$$T(x', \psi, \epsilon = -1, f_\kappa) = T(x)\left(1 + \frac{v_\Psi^2}{\kappa w_c^2}\right) . \quad (30a)$$

Equation (30a) is the macroscopic restatement of the microscopic conservation of energy and replaces the Bernoulli conservation law of equation (9) when no mass flux is present. It may be reshaped into a recognizable form that looks like a conserved Lagrangian per unit density:

$$T(x') - \frac{2}{2\kappa - 3}\psi(x') = L . \quad (30b)$$

Equation (30a) mathematically restates the effect of velocity filtration for the kappa model nonthermal boundary distribution: provided that the boundary distribution is nonthermal ($\kappa < \infty$),

the temperature increases with the potential energy stored, reflecting the systematic exclusion of the lowest energy particles from locales of higher potential energy.

For a distribution at rest with kappa distribution boundary condition in a monotonic attractive potential, equations (28) and (29) imply that the equation of state is a polytrope of the form

$$P(x', \psi, \epsilon = -1, \mu = 0) \propto N(x', \psi, \epsilon = -1, \mu = 0)^{\gamma}, \quad (31a)$$

$$\gamma(U = 0, \epsilon = -1, \kappa, 1D) = \frac{2\kappa - 1}{2\kappa + 1} < 1, \quad \kappa < \infty . \quad (31b)$$

Like Figure 10, Figure 12 shows that the numerical results of P and N variations induced by ψ (using the results of § 4 for a given κ function boundary condition) does obey the predicted polytrope's functional dependence on κ given by equation (31b). The solid curve is that predicted by equation (31b), while the asterisks are the results of the direct numerical integration and least-squares procedure discussed above to determine $(d \ln P/d\psi)/(d \ln N/d\psi)|_{\kappa}$. The agreement is nearly perfect, with slight discrepancies clearly traced to finite machine precision effects in the numerical integration of equations of the form of equation (12).

A three-dimensional phase space interacting in the same monotonic attractive potential along an isomagnetic tube of force also yields a polytrope relation with a slightly different index that is also less than unity, viz.,

$$\gamma(U = 0, \epsilon = -1, \kappa, 3D) = \frac{2\kappa - 3}{2\kappa - 1} < 1, \quad \kappa < \infty . \quad (31c)$$

The general case including magnetic field strength variation (cf. Paper II) does *not* yield a polytrope variation but does demonstrate that "heating" remains the prediction of the attractive case as graphically suggested in § 2.

In the case of both equations (31b) and (31c), $\gamma < 1$, and the effective logarithmic derivative of temperature with respect to density in such regimes is negative definite, suggesting that the temperature goes up as the density goes down, as shown in Figure 4. The strength of that anticorrelation increases as the suprathermal strength on the boundary increases (i.e., as κ decreases). In order for the kappa distribution to have a finite pressure, certain limits on κ must be observed: in a one-dimensional gas κ must exceed $\frac{1}{2}$, and in a three-dimensional phase space κ must be bigger than 3/2, yielding a lower bound on the polytrope exponent of zero. In the Maxwellian limit, $\kappa \to \infty$ and equations (31b) and (31c) recover the isothermal exponential atmosphere behavior illustrated in Figure 3 and derived in equation (27b). *This analysis demonstrates the singular behavior of the Maxwellian boundary condition interacting with decelerating forces, and shows that new effects of "velocity filtration" are possible if astrophysically ubiquitous suprathermal tail formation is allowed to be present in the boundary condition.*

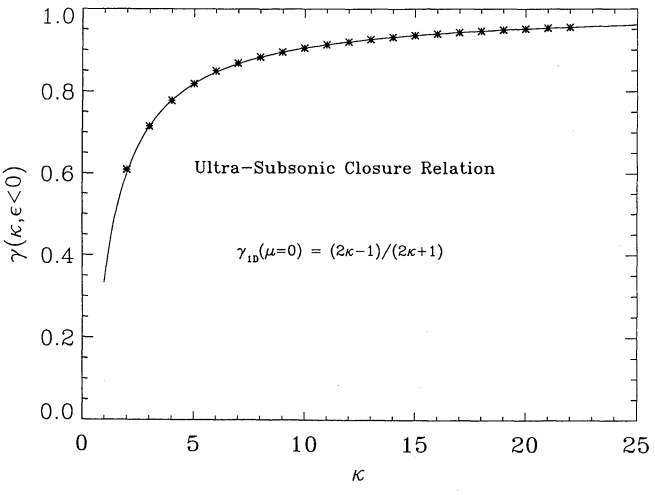

FIG. 12.—Polytrope verification. Comparison of theoretical ultra-subsonic polytrope expectation (eq. [30b]) with results of numerical integration.

For any suprathermal distribution (such as a kappa distribution with a finite κ) these results suggest that the temperature at the base of the collisionless expansion of stellar plasma envelopes should increase as the density decreases at the "edge" of the star. In the subsonic limit velocity filtration induces correlations so that $-1 < d \ln T/d \ln n \leq 0$. This suggestion is developed more completely in Paper II, which follows this paper in this issue.

As argued above, the consideration of a given potential and hence a given change in the density depends on preparing the boundary distribution appropriately so that a steady state is consistently permitted and the FIPH prerequisites are met. In general, each point that makes up the matrix of points contoured in the lower panels of Figures 8*a*–8*c* and 9*a*–9*c* is the result of a comparison with the moment over a *different* boundary function for each value of the attractive potential assumed; this can be seen for attractive potentials, because the trapping region of f_B in Figure 6 must change to be consistent with a steady state (cf. eqs. [12] and [14]). Therefore, as the attractive ψ changes, a different f_B is usually required to preserve the Mach number invariance.

The $\mu = 0$ boundary distribution, $f_B(\mu = 0)$, is already symmetric about $v = 0$; it *may* be chosen as the *same* even function, f_{κ}, of v at $x = 0$ for *any* size attractive potential. In this situation, as the potential increases, the distribution function on the trapped characteristics $[f(v, x = 0), |v| < v_{\phi}]$ *need not change* to be consistent with a steady state solution. This should be contrasted with a Mach 1 boundary distribution of the form given by f_{κ}, where the symmetrized portion of f_B at $x = 0$ for $v < v_{\Psi}$ must change as v_{Ψ} increases to be consistent with a steady state. For very high Mach number flows ($\mu \gg 1$) the boundary distribution for modest potentials does not have any significant overlap with the $E < \Delta\psi$ characteristics, allowing an approximate equation of state as derived in equation (23a) and (23b).

Because equations (13)–(15) are continuous functions of μ, the analytically obtained behavior for $\mu = 0$ is expected for small Mach number subsonic flows, provided that a consistent approach for f_B is adopted. Referring back to the general solution topology of Figures 8*a* and 9*a*, we see that the behavior at small Mach number is that expected from the analysis, namely, heating for attractive potentials for $\kappa = 2$ and virtually isothermal for the nearly Maxwellian regime of $\kappa = 24.9$. Quantitatively the heating ratios are smaller than implied by equation (30a) at small Mach numbers in Figures 8 and 9, because even as $\mu \to 0$ the *method of filling* the trapped particles in the Vlasov problem ($f_{\text{trapped}} = C$) as outlined in § 4 *is not continuous* with the method required for FIPH and used in § 5 for the heating estimates where $f_{\text{trapped}} = f_{\kappa}$. Physically the origin of this trapped population in the case of the solar problem is that of

the photospherical collisional bath. Finite Mach number boundary distributions with $f_{\text{trapped}} = f_\kappa$ also illustrate that "heating" comparable to that reported in equation (30a) is achieved.

The polytrope formulation of this section is only appropriate for spatially monotonic potential profiles, and then only for slow bulk flows with species Mach numbers small compared with unity and for distributed potentials along isomagnetic tubes of force. In the case of closed isomagnetic coronal configurations, equilibria with no flows can be envisaged (cf. Paper II, Fig. 6), and hence the polytrope behavior is expected throughout the entire loop. In the open topology of a coronal hole, where the medium is still ultra-subsonic, one expects the density and temperature profile to be initially anticorrelated. The open topology with a mass flux requires an energy drain per particle from internal energy and potential energy into flow and conduction energy to be consistent with the Bernoulli equation (eq. [9]). Ultimately tubes of force that connect the photosphere to the corona have large changes in B and new effects to consider. Because of the changes in the electrical potential, the equivalent proton potential is clearly nonmonotonic (Jockers 1970) at or near the sonic point (cf. Scudder 1992b), of the expansion, near some inferred estimates of the temperature maximum (cf. Munro & Jackson 1977; Lallement, Holzer, & Munro 1986). Thus, the anticorrelation between T and n derived here for the ultra-subsonic case should no longer be expected beyond this point. The ambipolar coupling of the electrons and ions implies that when the closure approximation for ions outlined here breaks down there too, the expectations for the electron profile should change. Finally, it should be emphasized that the polytrope behavior of ions and electrons will probably be different, because they experience different equivalent potentials and may also have different suprathermal distributions as boundary conditions (cf. Paper II).

Although Coulomb collisions are always present, they can sometimes be finessed in first approximation as was done here in the FIPH configuration for attractive potentials. Several mitigating factors are that Coulomb collisions are most frequent for the lowest kinetic energy particles; in the attractive case these are always $E \leq \Delta\psi$ particles already symmetrized in the prepared states of the initial data. Hence, the collisions, in first approximation, make an already symmetric nearly Maxwellian shape distribution (in the subsonic case) more so; the dearth of collisions at suprathermal kinetic energies implies that the existence of collisions per se does not interfere with the free-streaming effects outlined above. At lower energies where the momentum exchange is most important, minor phase-space modifications will occur, such as bringing the thermal electrons to move nearly at the bulk speed of the ions. This effect represents a very minor modification to the overall gross rearrangement of random kinetic energy that the reversible potentials can induce. Both of these effects would appear perturbatively accessible once the lowest order Knudsen effects of the FIPH obtained here were understood. An example of this a posteriori assessment of the quantitative importance of collisional effects in the transition region and low corona is presented in Paper II.

6. DISCUSSION

In a plasma without collisions, or in a FIPH approach with collisions, the time-independent, coherent Vlasov behavior of the particles in the presence of spatially varying conservative force fields can modify the electron and ion temperatures. The particle velocity distributions need not be horribly deformed under such Vlasov evolution, especially in an attractive case where boundary distributions were selected to resemble those that can be made from collisions. Inasmuch as the "widths" of these distributions affect any remote astrophysical diagnostic sensitive to the width of the random distribution of the plasma constituents, the qualitative behavior illustrated here will cause almost the same types of effects as a Maxwellian of equivalent density and temperature (cf. Paper II, Figs. 12*a* and 12*b*). Therefore, these reversible forces can affect the interpretation of remote diagnostics that are frequently used to infer temperature increases that, in turn, are used to infer entropy production. The existence of the suprathermal tails will, however, influence the quantitative shape of Doppler-broadened lines (cf. Paper II), the population of states, and the statistical mechanics that gets built into many astrophysical calculations and conclusions.

Interactions with potentials were demonstrated where the plasma was either cooled or heated. In most cases a plasma is heated as a result of the interaction with a potential. Counterexamples are (1) Maxwellians at rest interacting with attractive potentials whose temperatures are unmodified and (2) supersonic distributions that are cooled when accelerated by a repulsive potential. A general result has been established for spatially monotonic attractive potentials in the presence of non-Maxwellian boundary distributions: *although the statistical description is isentropic, the spatial temperature and density profiles will be anticorrelated.*

The theoretical effects discussed here have been observed with *in situ* spacecraft and laboratory phase-space measurements as summarized in Figure 13. The accelerating subsonic collisionless case is witnessed in the "heating" or "inflation" of the electron velocity space in the accelerating deHoffmann–Teller electric field at the Earth's bow shock (Scudder et al. 1986c). The accelerating supersonic case is a well-known laboratory regime in electron-ion beam optics for making the beam more monoenergetic, hence cooler. The decelerating supersonic case is much like the initial interaction of the supersonic ions of the solarwind with the normal incidence frame (Goodrich & Scudder 1984) cross-shock electric field observed in particle simulations reported by Leroy et al. (1981) and documented, for example, in Scudder et al. (1986a, b). Finally, the attractive potential's deceleration of an ultra-subsonic electron gas occurs at the Earth's magnetopause (Scudder 1989). Much as in Figure 4*c*, the lowest energy electrons of the nonthermal magnetosheath distribution are filtered out of the magnetopause cavity, leaving the more energetic and higher mean energy particles to precipitate onto the polar cap as the "polar rain" (Fairfield & Scudder 1985; Baker et al. 1986; Scudder 1989). Even after giving up the kinetic energy to overcome this voltage drop at the magnetopause, the *mean* energy of the remaining precipitating electrons is enhanced over the mean energy of the magnetosheath spectrum by velocity filtration. As predicted above, the flux of the precipitating polar rain electrons is anticorrelated with the mean energy (temperature) as reported, for example, in Riehl & Hardy (1986); this in turn implies that the number density and mean energy are also anticorrelated as expected by the velocity filtration mechanism. As a by-product of arguments that the polar rain electron distributions are filtered remnants of the coronal exobase, observational data are now available to suggest that the coronal velocity distribution of electrons does

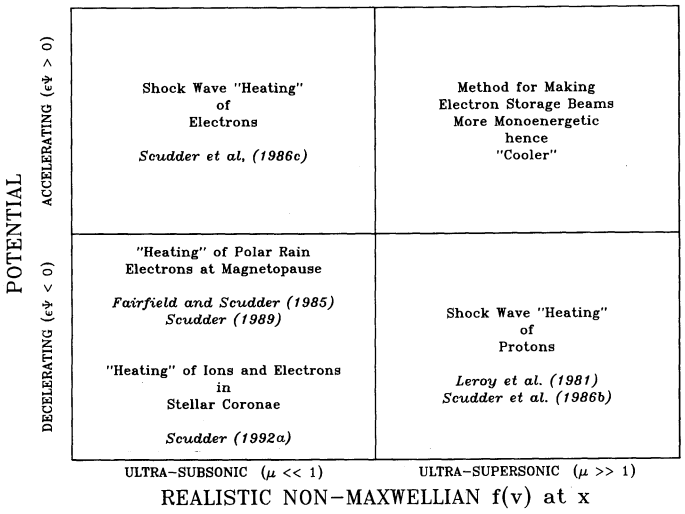

FIG. 13.—Experimental evidence of temperature change at x'. Reversible potentials as explanations for observations of *in situ* astrophysical plasma observations; these systems and their diagnosis represent the "ground truth" of the theoretical ideas discussed in this paper. They and the theory provide a framework for new understanding in remote astrophysical systems.

routinely have a suprathermal tail (Fairfield & Scudder 1985; Riehl & Hardy 1986). A further mysterious anticorrelation between the *ion* temperature and density in the Earth's central plasma sheet has been recently reported (Huang et al. 1989). It, too, may reflect the energy-dependent threshold of access of suprathermally overpopulated ions as they refill the plasma sheet of the Earth's magnetotail.

In the ultra-supersonic regime a one-dimensional phase-space gas is shown to behave as an anisotropic gas, behaving almost as if it were a one dimensional adiabatic gas in the direction of the applied acceleration.

Prototype nonthermal ultra-subsonic boundary distributions in monotonic attractive potentials distributed along isomagnetic tubes of force have been shown to obey a polytrope law with exponent $\gamma < 1$. This exponent has no analog in gas dynamics. *The type of closure* $(0 < \gamma < 1)$ *the present calculation discloses would never have been explored by modelers who "borrow" polytrope closure expressions for convenience and explore only those regimes of polytrope exponent familiar from neutral gas kinetic theory of* $1 \leq \gamma \leq 5/3$. In particular, conventional polytrope models of systems undergoing expansion are always drawn to the addition of heat to provide a temperature profile that increases as the density decreases. The present model calculations have demonstrated that the addition of heat is not an inescapable conclusion. Having explored all polytropic regimes within the range $1 \leq \gamma \leq 5/3$, the modeler has *not* surveyed the entire spectrum of possibilities, especially when nonthermal distributions are conceivable at the boundaries of the problem at hand!

The present calculations illustrate that the *polytrope simplifications* of kinetic behavior, *if possible, are situation-dependent* and generally do *not* reflect *an intrinsic property of the gas independent of space.* The precise value of γ has been determined to be a function of the species change and mass, modeled nonthermal tail strength, sign of force, local topology of the potential, Mach number, as well as the assumed boundary distribution function. The relevant γ is derived on the higher authority of kinetic theory and has been determined as a function of the strength of the nonthermal tails of the boundary distribution function. In the limit where the boundary distribution is a Maxwellian at rest, the analytic form of $\gamma(\kappa \to \infty)$ approaches unity, recovering the well-known isothermal response of the Maxwellian to attractive potentials, which underlies the well-known exponential atmosphere.

When the nonlocal effects are present as discussed in this paper, no general theorem is known that states that the relationship between density and temperature will be polytropic either for the plasma as a whole, or for either or both ions and electrons separately; in general it would not seem possible that such a restricted functional *Ansatz* is broad enough for all forms of closure possible in the presence of the global nonlocal effects that can modify the temperature. Two limiting forms have been presented that were amenable to such a functional reduction. By studying how the polytrope is possible, new insight has been gained about the way interactions between previous disjoint reservoirs of energy have been realized. There may exist other unexplored paths for producing temperature inversions, for example, without actually depositing heat in the locales where the temperature is desired to increase.

General graphical constructions have been presented for attractive potentials to show that distributions with suprathermal tails will evolve spatially in a way similar to those distributions amenable to closed-form calculation. *While polytropes may not be the general functional equation of state for monotonic attractive potentials, the anticorrelation between T and n implied by such calculations are suggested to be generic for all suprathermal boundary distributions.*

General rules of expected behavior for a Vlasov or FIPH gas of differing Mach numbers interacting with a spectrum of reversible forces are shown in Figures 14*a* and 14*b* for Maxwellian and suprathermal boundary conditions, respectively. Effects such as these can strongly influence astrophysical measurements. These qualitative rules, together with a gross knowledge of the forces involved, may help include or discount the

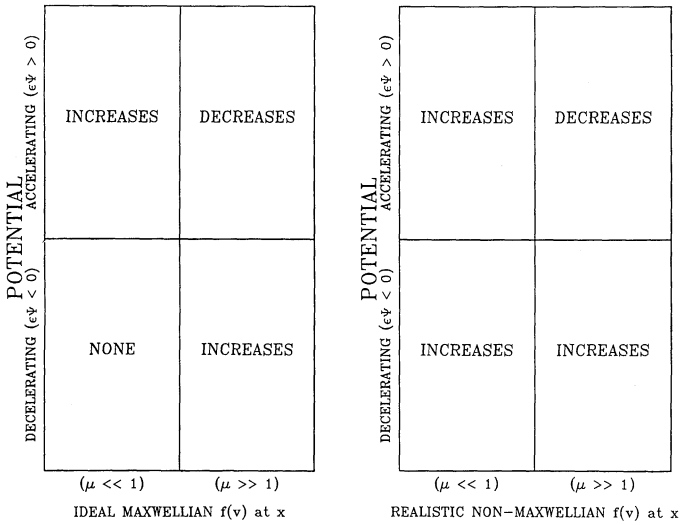

FIG. 14.—Temperature change at x'. Summary of general rules of expected temperature changes for (*left*) Maxwellian boundary conditions and (*right*) realistic distributions with suprathermal populations interacting with all combinations of ultra-subsonic, supersonic, and attractive and repulsive potentials.

importance of these effects in the best inversion and interpretation of the sparse and convolved remote astrophysical observations.

The information concerning the presence of suprathermal tails is found in the fluid moments of level 4 and above. The truncation at level 2 of the infinity of coupled fluid moment equations made possible by the Spitzer-Braginskii approach presupposes the unimportance of suprathermal features of the velocity distribution function. The calculations of this paper and Paper II that follows strongly suggest that such truncations are overly restrictive and should be relaxed when describing astrophysical plasmas.

Discussions with L. F. Burlaga are acknowledged; he, D. Deming, and A. Klimas of the NASA–GSFC Laboratory of Extraterrestrial Physics and D. Reames of the NASA–GSFC Laboratory for High Energy Astrophysics have also made helpful and detailed comments on an earlier version of the paper. The comments of the referee are also acknowledged.

REFERENCES

Baker, D. N., et al. 1986, J. Geophys. Res., 91, 5637
Boltzmann, L. 1875, Wien. Ber., 72, 427
Braginskii, S. 1965, in Rev. Plasma Phys., 1, 205
Bridge, H. S., et al. 1974, Science, 185, 4131
Cercignani, C. 1975, Theory and Application of the Boltzmann Equation (New York: Elsevier)
Chandrasekhar, S. 1939, Stellar Structure (New York: Dover)
Chapman, S. 1916, Proc. Soc. London, A, 216, 279
Chapman, S., & Cowling, T. G. 1970, The Mathematical Theory of Non-uniform Gases (Cambridge: Cambridge Univ. Press)
Christon, S. P., Williams, D. J. Mitchell, D. G., Huang, C. Y., & Frank, L. A. 1991, J. Geophys. Res., 96, 1
Cuperman, S., Weiss, I., & Dryer, M. 1980, ApJ, 329, 345, 1980
deGroot, S. R., & Mazur, P. 1984, Non-equilibrium Thermodynamics (New York: Dover)
Delettrez, J. 1985, Canadian J. Phys., 64, 932
Enskog, D. 1917, Ph.D. thesis, Uppsala Univ.
Fairfield, D. H., & Scudder, J. D. 1985, J. Geophys. Res., 90, 4055
Feldman, W. C., Asbridge, J. R., Bame, S. J., & Montgomery, M. D. 1973, J. Geophys. Res., 78, 2017
Feldman, W. C., Asbridge, J. R., Bame, S. J., Montgomery, M. D., & Gary, S. P. 1975, J. Geophys. Res., 80, 4181
Goodrich, C. C., & Scudder, J. D. 1984, J. Geophys. Res., 89, 6654
Hartle, R. E., Sittler, E. C., Ogilvie, K. W., Scudder, J. D., & Lazarus, A. J. 1982, J. Geophys. Res., 87, 1383
Huang, C. Y., Goertz, C. K., Frank, L. A., & Rostoker, G. 1989, Geophys. Res. Lett., 16, 563
Jockers, K. 1970, A&A, 6, 219
Krimigis, S. M., et al. 1981, J. Geophys. Res., 86, 8227
Lallement, R., Holzer, T., & Munro, R. H. 1986, J. Geophys. Res., 91, 751
Leroy, M., Goodrich, C. C., Winske, D., Wu, C. S., & Papadopoulos, K. 1981, Geophys. Res. Lett., 8, 1269
Marsch, E., & Goldstein, H. 1983, J. Geophys. Res., 88, 9933
Maxwell, J. C. 1873, Nature, 8, 537
Montgomery, M. D. 1972, in Cosmic Plasmas, ed. K. Schindler (New York: Plenum)
Montgomery, M. D., Bame, S. J., & Hundhausen, A. J. 1968, J. Geophys. Res., 73, 4999
Munro, R. H., & Jackson, B. V. 1977, ApJ, 213, 874
Ogilvie, K. W., et al. 1974, Science, 185, 4146
Ogilvie, K. W., Scudder, J. D., & Sugiura, M. 1971a, J. Geophys. Res., 76, 3574
———. 1971b, J. Geophys. Res., 76, 8165
Ogilvie, K. W., Scudder, J. D., Vasyliunas, V. M., Hartle, R. E., & Siscoe, G. L. 1977, J. Geophys. Res., 82, 1807
Olbert, S. 1969, in Physics of the Magnetospheres, ed. R. C. Carovillano, J. F. McClay, & H. R. Radoski (Dordrecht: Reidel), 641
———. 1983, in Solar Wind 5, ed. M. Neugebauer (NASA CP-2280), 149
Olbert, S., Egidi, A., Moreno, G., & Pai, L. G. 1968, Trans. AGU, 48, 177
Owocki, S. P., & Scudder, J. D. 1983, ApJ, 270, 758
Parker, E. N. 1958, ApJ, 128, 664
———. 1964a, ApJ, 139, 72
Riehl, K., & Hardy, D. A. 1986, J. Geophys. Res., 91, 1557
Rosenbauer, H., Miggenreider, H., Montgomery, M., & Schwenn, R. 1976, in Physics of Solar Planetary Environments, ed. D. J. Williams (Washington, DC: AGU), 319
Rosenbluth, M., Macdonald, W. M., & Judd, D. L. 1957, Phys. Rev., 107, 1
Rossi, B., & Olbert, S. 1970, Introduction to the Physics of Space (New York: McGraw-Hill), 324
Scudder, J. D. 1987a, Trans. AGU, 68, 381
———. 1987b, invited talk at Balatonfüred Collisionless Shock Conf.
———. 1989, Trans AGU, 70, 432
———. 1992a, ApJ, 398, 319 (Paper II)
———. 1992b, J. Geophys. Res., submitted
Scudder, J. D., et al. 1986a, J. Geophys. Res., 91, 11019
Scudder, J. D., Mangeney, A., Lacombe, C., Harvey, C. C., & Aggson, T. L. 1986b. J. Geophys. Res., 91, 11053
Scudder, J. D., Mangeney, A., Lacombe, C., Harvey, C. C., Wu, C. S., & Anderson, R. R. 1986c, J. Geophys. Res., 91, 11075
Scudder, J. D., Sittler, E. C., & Bridge, H. S. 1981, J. Geophys. Res., 86, 8157
Scudder, J. D., & Olbert, S. 1979a, J. Geophys. Res., 84, 2755
———. 1979b, J. Geophys. Res., 84, 6603
———. 1983, in Solar Wind 5, ed. M. Neugebauer (NASA CP-2280), 163
Shoub, E. C. 1982, Stanford Inst. Plasma Phys. Rep., No. 46
———. 1983, ApJ, 226, 339
———. 1989, in Proc. Sixth Int. Solar Wind Conf. I, ed. V. Pizzo, T. E. Hozer, & D. Sime (Boulder: NCAR/TN-306), 59
Sittler, E. C., Scudder, J. D., & Bridge, H. S. 1981, Nature, 292, 711
Spitzer, L., & Härm, R. 1953, Phys. Rev., 80, 977
Tait, J. 1886, Edinburgh Trans., 33, 74
Vasyliunas, V. 1968, J. Geophys. Res., 9, 2839